Hydrodynamics and CP_2 Geometry

M. Pitkänen,

February 2, 2024
Email: matpitka6@gmail.com.
http://tgdtheory.com/public_html/.
Postal address: Rinnekatu 2-4 A 8, 03620, Karkkila, Finland. ORCID: 0000-0002-8051-4364.

Contents

Abstract

The chapter is one of the earliest attempts to apply TGD to macroscopic physics and must be taken as such. The chapter begins with a brief summary of the basic notions related to many-sheeted space-time. A generalization of hydrodynamics to a p-adic hierarchy of hydrodynamics is considered and a mechanism of energy transfer between condensate levels is identified. It is suggested that TGD based generalization of Hawking-Bekenstein law holds even in macroscopic length scales and that hydrodynamical vortices behave in some aspects like elementary particles. TGD leads to a formulation of a general theory of phase transitions: the new element is the presence of several condensate levels.

It has much later become clear that the vision about elementary particles Euclidian space-time regions defining lines of generalized Feynman diagrams generalizes to macroscopic scales and that every macroscopic body should accompany such space-time sheet and thus in some aspects behave like elementary particle.

A topological model for the generation of the hydrodynamical turbulence is proposed. The basic idea is that hydrodynamical turbulence can be regarded as a spontaneous Kähler magnetization leading to the increase the value of Kähler function and therefore of the probability of the configuration. Kähler magnetization is achieved through the formation of a vortex cascade via the decay of the mother vortex by the emission of smaller daughter vortices. Vortices with various values of the fractal quantum number and with sizes related by a discrete scaling transformation appear in the cascade. The decay of the vortices takes place via the so called phase slippage process.

An encouraging result is the prediction for the size distribution of the vortices: the prediction is practically identical with that obtained from the model of Heisenberg but on rather different physical grounds. The model is rather insensitive to the p-adic scaling of vortices in the transition as long as it is smaller than $\lambda = 2^{-5}$. The model is also consistent with the assumption that the decay of a vortex to smaller vortices corresponds to a phase transition from a given level of dark matter hierarchy to a lower level so that the value of $\hbar$ is reduced by a factor $\lambda = v_0/n \simeq 2^{-11}/n$, $n = 1, 2, ...$ so that Compton length scales as well as sizes of vortices are reduced by this factor.

1 Introduction

The understanding of the turbulence is a longstanding problem in hydrodynamics [B4, B3]. This problem is acute also in astrophysics [E3]. where the proper understanding of the turbulence associated with the astrophysical systems, such as the mass accretion in a binary star, is lacking. A generally accepted point of view is that Navier-Stokes equations provide a correct description of the hydrodynamics and that the problems are of purely technical nature, being analogous to the difficulties encountered in the understanding of the color confinement.

1.1 Basic Ideas And Concepts

TGD approach to the description of the fundamental interactions suggests a fresh approach to the basic problems of the hydrodynamics. The new physical ideas are the following ones.

1.1.1 The notion of topological condensate

The concept of topological condensate: the criticality of the Kähler function and topological arguments suggest that 3-space has many-sheeted, fractal like, hierarchical structure consisting of 3-surfaces with boundary, topological field quanta, condensed on larger topological field quanta. The n:th level of the topological condensate is characterized by a length scale $L(n)$ giving lower bound for the size of the topological quanta at this level.

Various gauge fluxes and gravitational flux associated with a given topological field quantum flow to the lower condensate level via # contacts near the boundaries of the topological field quanta, whose microscopic description in terms of partons is discussed in [**?**]. The outer surfaces of the macroscopic bodies are identified as the boundaries of the topological field quanta condensed in the background 3-space.

Topological field quanta are characterized by certain vacuum quantum numbers and the space-time in the astrophysical length scales corresponds to the large vacuum quantum number limit of TGD. In the present situation hydrodynamic vortex provides a good candidate for a topological

field quantum condensed on the background 3-space and at a given level vortices must have size not smaller than the length scale $L(n)$. Actually this picture of the space-time requires the generalization of the ordinary hydrodynamics to a hierarchy of hydrodynamics, one for each condensate level and also the modelling of the energy transfer between various condensate levels. In this chapter only the modifications of the hydrodynamics associated with a given condensate level are considered.

The join along boundaries bond makes it possible to glue topological field quanta together to form a larger coherent quantum systems from simpler basic units. Since dissipation corresponds to a loss of the quantum coherence, the formation of the join along boundaries bonds should play a key role in the understanding of the dissipation, in particular hydrodynamic dissipation.

A concrete topological description for the dissipation is following. The basic mechanism of the dissipation at condensate level n are the inelastic collisions of the condensed topological field quanta involving the formation and splitting of the join along boundaries bonds and leading to the transfer of the kinetic energy to the kinetic energy of the topological field quanta at higher condensate level n_1 with $L(n_1) < L(n)$. Eventually the kinetic energy of the flow ends up to the atomic condensate levels, where the collisions of atoms take care of the dissipation. The modelling of this mechanism requires a model for the coupling between hydrodynamics associated with two different condensate levels.

It has much later become clear that the vision about elementary particles Euclidian space-time regions defining lines of generalized Feynman diagrams generalizes to macroscopic scales and that every macroscopic body should accompany such space-time sheet and thus in some aspects behave like elementary particle.

1.1.2 Long range color and electroweak gauge fields created by dark matter

TGD predicts classical long ranged color and weak forces, in particular Z^0 force. The study of the imbeddings for various metrics [K14] suggests strongly that at long length scales matter is accompanied by long range electro-weak gauge fields. For vacuum extremals em field can vanish while Z^0 field is non-vanishing: this requires that Weinberg angle satisfies $sin^2(\theta_W) = 0$ in this phase. In the astrophysical length scales Z^0 charge is proportional to the gravitational mass of the system, when Planck mass is used as unit: $Q_Z = \epsilon_1 m/m_{Pl}$, where ϵ_1 is numerical factor smaller.

Also long ranged classical W fields are possible as well as classical long ranged color fields. The proper interpretation is in terms of scaled down hierarchy of weak and color physics assignable to a hierarchy of dark matters coupling to ordinary matter only via gravitation directly. These physics manifest themselves already in nuclear physics [K12] and condensed matter physics [K8]. in particular in the physics of living matter. The appearance of classical Z^0 fields in the bio-systems could explain chirality selection in the living matter.

TGD based model for atomic nuclei predicts that nucleons are connected by color bonds connecting exotic quarks with mass of order MeV. These quarks couple to light variants of weak bosons with Compton length of order atomic radius so that the range of these exotic weak forces would be about atomic radius. These color bonds can have also net em and weak charges so that nucleus develops an anomalous weak charge. More generally, a hierarchy of scaled up variants of weak and color physics is predicted and the range 10 nm-2.5 μm containing the electron Compton lengths $L_e(k) = \sqrt{5}L(k)$ associated with four Gaussian Mersennes is especially interesting in this respect.

As a consequence, the dark matter part of condensed matter system serves as a source of Z^0 electric and magnetic fields. These fields are vacuum screened above the relevant weak length scale L_w. This means that the space-time sheets of weak bosons are of size L_w and weak gauge fluxes are not conserved in # contacts to larger space-time sheets. The outcome is randomness and loss of coherence in length scales longer than L_w.

In particular, moving matter at given dark space-time sheet creates Z^0 magnetic field

$$\nabla \times B_Z \quad \simeq \quad g_Z N \beta \ . \tag{1.1}$$

where N is the density of weak isospin of dark matter using neutrino isospin as a unit. This formula makes sense below the appropriate weak length scale determined by the mass of dark weak bosons in question. Above this length scale vacuum screening occurs. Z^0 electric field satisfies also the appropriate source equation.

Although the Z^0 fields as such are extremely weak, the topological obstructions caused by the CP_2 topology for the imbeddings of the Z^0 magnetic fields are nontrivial. CP_2 topology generates structures: the hydrodynamical flow decomposes into what could be called flux quanta of the Z^0 magnetic field. It will be later found that under rather natural assumptions the sizes of the flux quanta are indeed of the same order of magnitude as the sizes of the typical structures associated with the hydrodynamic flow. In particular, for large systems typically encountered in astrophysics, the geometry of CP_2 is bound to become important.

Around 2004 the idea about hierarchy of Planck constants explaining dark matter emerged. Since weak scale is proportional to h_{eff}, the prediction is that it could be even macroscopic for large enough value of h_{eff}. Around 2012 the realization that the modes of induced spinor field are localized to 2-D surfaces in generic case. Induced W fields and possibly also Z^0 fields vanish at these surfaces so that strong parity breaking effects are not present.

1.2 Z^0 Magnetic Fields And Hydrodynamics

In [K12] long ranged color and weak forces associated with the color bonds between nucleons inside atomic nuclei are proposed as an explanation for the basic properties of the ordinary liquid phase and for the anomalous characteristics of liquid water. The mathematical similarity between incompressible hydrodynamical flow and Maxwell equations for magnetic field forces to ask whether Z^0 magnetic fields created by the dark matter component of condensed matter system might provide deeper insights into the physics of hydrodynamical flow. The general study of solutions of field equations [K2] indeed leads to very general mathematical insights in this respect providing a classification of asymptotic flow patterns in terms of the dimension of CP_2 projection varying in the range $2 \leq D \leq 4$.

1.2.1 Z^0 magnetic fields and transition to turbulence

The concept of the Z^0 magnetic field suggests a new approach to the problem of understanding how the transition to turbulence takes place. The transition to a turbulence might be understood simply as a spontaneous Z^0 magnetization. Flow decomposes into eddies carrying a Z^0 magnetic field in the direction of the rotation axis of the eddy. Due to the viscosity, the size of the eddy grows until its size becomes critical. Vortices dissipate their energy and angular momentum by the emission of daughter vortices: the emission is a generalization of the process known as a phase slippage in super fluidity [D3]. This mechanism suggests fractal like structure for the development of the hydrodynamic turbulence. In fact, it will be found CP_2 geometry implies naturally fractal like structures [A1] and the model for the turbulence relies heavily on the assumption that the sizes of the daughter eddies are related to the size of the mother eddy by a discrete scaling transformation.

1.2.2 Turbulence and Z^0 magnetization

TGD suggests a first principle explanation for the occurrence of a spontaneous Z^0 (and Kähler) magnetization and therefore of turbulence. The probability of the configuration is proportional to the exponent of the Kähler function. Kähler function corresponds to the absolute minimum of the Kähler action and Kähler magnetic (electric) fields give a positive (negative) contribution to the Kähler action so that a transition to a configuration containing Kähler magnetic fields can take place provided the configuration is energetically possible and corresponds to the minimum of Kähler action.

It turns out that for a certain critical values of the flow parameters, Kähler magnetization takes place and implies the generation of the eddies and turbulence. The mechanism leading to the increase of the Kähler action is however not the generation of magnetic Kähler action but the decrease of the magnitude of the Kähler electric contribution as is understandable from the fact that Kähler magnetic fields of the flow are in general by a factor β (β is the typical flow velocity) weaker than the Kähler electric fields. The decrease of the Kähler electric contribution follows from the fact that the Kähler electric field of the vortex becomes small near the core of the vortex. It should be noticed that a similar explanation might apply to other types of phase transitions, say spontaneous magnetization.

1.3 Topics Of The Chapter

The topics of the chapter are following.

1. The chapter begins with an updated review of the basic aspects of the many-sheeted space-time concept.

2. Hydrodynamical and thermodynamical hierarchies associated with the p-adic length scale hierarchy are considered. A generalization of hydrodynamics to a p-adic hierarchy of hydrodynamics is performed and a mechanism of energy transfer between condensate levels is identified. Mary Selvam has found a fascinating connection between the distribution of primes and the distribution of vortex radii in turbulent flow in atmosphere. These observations provide new insights into p-adic length scale hypothesis and suggest that TGD based generalization of Hawking-Bekenstein law holds even in macroscopic length scales and that hydrodynamical vortices behave in some aspects like elementary particles.

3. General ideas about the description of phase transitions in terms of configuration space geometry (configuration space understood as the space of 3-surfaces, the "world of classical worlds") are considered. The new element is the presence of several condensate levels.

4. Some simple cylindrically symmetric flows are studied and it is shown that the sizes of the flux structures are of a correct order of magnitude under rather natural assumptions about the vacuum parameters characterizing electrovac neutral space-time.

5. A detailed model for the generation of turbulence as a spontaneous Kähler (implying both em and Z^0 magnetization) magnetization in the case of the channel flow is discussed.

An encouraging result is the prediction for the size distribution of the vortices: the prediction is practically identical with that obtained from the model of Heisenberg but on rather different physical grounds. The model is rather insensitive to the p-adic scaling of vortices in the transition as long as it is smaller than $\lambda = 2^{-5}$. The model is also consistent with the assumption that the decay of a vortex to smaller vortices corresponds to a phase transition from a given level of dark matter hierarchy to a lower level so that the value of $\hbar$ is reduced by a factor $\lambda = v_0/n \simeq 2^{-11}/n$, $n = 1, 2, ...$ so that Compton length scales as well as sizes of vortices are reduced by this factor.

The appendix of the book gives a summary about basic concepts of TGD with illustrations. There are concept maps about topics related to the contents of the chapter prepared using CMAP realized as html files. Links to all CMAP files can be found at `http://tgdtheory.fi/cmaphtml.html` [**?**]. Pdf representation of same files serving as a kind of glossary can be found at `http://tgdtheory.fi/tgdglossary.pdf` [**?**].

2 Many-Sheeted Space-Time Concept

In this section the basic phenomenology related to the many-sheeted space-time concept (see **Fig.** `http://tgdtheory.fi/appfigures/manysheeted.jpg` or **Fig.** 9 in the appendix of this book) is introduced. In [**?**] a more refined and more up-to-date review of these notions relying on number theoretic vision can be found. The vision about the role of dark matter in condensed matter and living matter is summarized in [K8].

2.1 Basic Concepts Related To Topological Condensation And Evaporation

The most up-to-date discussion of the notions such as topological condensation and evaporation, gauge charges, transfer of gauge field between different space-time sheets, ... can be found in [**?**].

2.1.1 CP_2 type vacuum extremals

CP_2 type extremals behave like elementary particles (in particular, light-likeness of M^4 projection gives rise to Virasoro conditions). CP_2 type vacuum extremals have however vanishing four-momentum although they carry classical color charges. This raises the question how they can gain elementary particle quantum numbers.

In topological condensation of CP_2 type vacuum extremal a light-like causal horizon is created. Number theoretical considerations strongly suggest that the horizon carries elementary particle numbers and can be identified as a parton. The quantum numbers or parton would serve as sources of the classical gauge fields created by the causal horizon.

In topological evaporation CP_2 type vacuum extremal carrying only classical color charges is created. This would suggest that the scattering of CP_2 type vacuum extremals defines a topological quantum field theory resulting as a limit of quantum gravitation (CP_2 is gravitational instanton) and that CP_2 type extremals define the counterparts of vacuum lines appearing in the formulation of generalized Feynman diagrams.

2.1.2 # contacts as parton pairs

The earlier view about # contacts as passive mediators of classical gauge and gravitational fluxes is not quite correct. The basic modification is due to the fact that one can assign parton or parton pair to the # contact so that it becomes a particle like entity. This means that an entire p-adic hierarchy of new physics is predicted.

1. Formally # contact can be constructed by drilling small spherical holes S^2 in the 3-surfaces involved and connecting the spherical boundaries by a tube $S^2 \times D^1$. For instance, CP_2 type extremal can be glued to space-time sheet with Minkowskian signature or space-time sheets with Minkowskian signature can be connected by # contact having Euclidian signature of the induced metric. Also more general contacts are possible since S^2 can be replaced with a 2-surface of arbitrary genus and family replication phenomenon can be interpreted in terms of the genus.

   The # contact connecting two space-time sheets with Minkowskian signature of metric is accompanied by two "elementary particle horizons", which are light-like 3-surfaces at which the induced 4-metric becomes degenerate. Since these surfaces are causal horizons, it is not clear whether # contacts can mediate classical gauge interactions. If there is an electric gauge flux associated with elementary particle horizon it tends to be either infinite by the degeneracy of the induced metric. It is not clear whether boundary conditions allow to have finite gauge fluxes of electric type. A similar difficulty is encountered when one tries to assign gravitational flux to the # contact: in this case even the existence of flux in non-singular case is far from obvious. Hence the naïve extrapolation of Newtonian picture might not be quite correct.

2. Number theoretical considerations suggests that the two light-like horizons associated with # contacts connecting space-time sheets act as dynamical units analogous to shock waves or light fronts carrying quantum numbers so that the identification as partons is natural. Quantum holography would suggest itself in the sense that the quantum numbers associated with causal horizons would determine the long range fields inside space-time sheets involved.

3. # contacts can be modeled in terms of CP_2 type extremals topologically condensed simultaneously to the two space-time sheets involved. The topological condensation of CP_2 type extremal creates only single parton and this encourages the interpretation as elementary particle. The gauge currents for CP_2 type vacuum extremals have a vanishing covariant divergence so that there are no conserved charges besides Kähler charge. Hence electro-weak gauge charges are not conserved classically in the region between causal horizons whereas color gauge charges are. This could explain the vacuum screening of electro-weak charges at space-time level. This is required since for the known solutions of field equations other than CP_2 type extremals vacuum screening does not occur.

4. In the special case space-time sheets have opposite time orientations and the causal horizons carry opposite quantum numbers (with four-momentum included) the # contact would serve the passive role of flux mediator and one could assign to the contact generalized gauge fluxes as quantum numbers associated with the causal horizons. This is the case if the contact is created from vacuum in topological condensation so that the quantum numbers associated with the horizons define naturally generalized gauge fluxes. Kind of generalized quantum dipoles living in two space-times simultaneously would be in question. # contacts in the

ground state for space-time sheets with opposite time orientation can be also seen as zero energy parton-antiparton pairs bound together by a piece of CP_2 type extremal.

5. When space-time sheets have same time orientation, the two-parton state associated with the # contact has non-vanishing energy and it is not clear whether it can be stable.

2.1.3 $\#_B$ contacts as bound parton pairs

Besides # contacts also flux tubes (JABs, $\#_B$ contacts) are possible. They can connect outer boundaries of space-time sheets or the boundaries of small holes associated with the interiors of two space-time sheets which can have Minkowskian signature of metric and can mediate classical gauge fluxes and are excellent candidates for mediators of gauge interactions between space-time sheet glued to a larger space-time sheet by topological sum contacts and join along boundaries contacts. The size scale of the causal horizons associated with parton pairs can be arbitrary whereas the size scale of # contacts is given by CP_2 radius.

The existence of the holes for real space-time surfaces is a natural consequence of the induced gauge field concept: for sufficiently strong gauge fields the imbeddability of gauge field as an induced gauge field fails and hole in space-time appears as a consequence. The holes connected by $\#_B$ contacts obey field equations, and a good guess is that they are light-like 3-surfaces and carry parton quantum numbers. This would mean that both # and $\#_B$ contacts allow a fundamental description in terms of pair of partons.

Magnetic flux tubes provide a representative example of $\#_B$ contact. Instead of $\#_B$ contact also more descriptive terms such as join along boundaries bond (JAB), color bond, and magnetic flux tube are used. $\#_B$ contacts serve also as a space-time correlate for bound state formation and one can even consider the possibility that entanglement might have braiding of bonds defined by # contacts as a space-time correlate [K1].

The formation of join along boundaries bonds/flux tubes could become important at the quantum limit, when the thermal de Broglie wave length $\lambda_{th} = \frac{2\pi}{\sqrt{2Tm}}$ (roughly the minimal size for the p-adic 3-surface at which particle with thermal momentum $p = \sqrt{2Tm}$ can condense) is of same order of magnitude as average separation between particles. A tempting identification for the formation of the flux tubes is as Bose-Einstein condensation taking place at same temperature range.

For solids join along boundaries/flux tube binding energy E_{join} can be, at least partially, regarded as the reduction of kinetic energy resulting from the elimination of translational degrees of freedom in the join along boundaries bond. Also the de-localization energy of particles, say conduction electrons contributes to E_{join} (de-localization is made possible by the formation of bridges between p-adic blocks).

2.1.4 Topological condensation and evaporation

Topological condensation corresponds to a formation of # or $\#_B$ contacts between space-time sheets. Topological evaporation means the splitting of # or $\#_B$ contacts. In the case of elementary particles the process changes almost nothing since the causal horizon carrying parton quantum numbers does not disappear. The evaporated CP_2 type vacuum extremal having interpretation as a gravitational instanton can carry only color quantum numbers.

As # contact splits partons are created at the two space-time sheets involved. This process can obviously generate from vacuum space-time sheets carrying particles with opposite signs of energies and other quantum numbers. Positive energy matter and negative energy anti-matter could be thus created by the formation of # contacts with zero net quantum numbers which then split to produce pair of positive and negative energy particles at different space-time sheets having opposite time orientations. This mechanism would allow a creation of positive energy matter and negative energy antimatter with an automatic separation of matter and antimatter at space-time sheets having different time orientation. This might resolve elegantly the puzzle posed by matter-antimatter asymmetry.

The creation of # contact leads to an appearance of radial gauge field in condensate and this seems to be impossible at the limit of infinitely large space-time sheet since it involves a radical

instantaneous change in field line topology. The finite size of the space-time sheet can however resolve the difficulty.

If all quantum numbers of elementary particle are expressible as gauge fluxes, the quantum numbers of topologically evaporated particles should vanish. In the case of color quantum numbers and Poincare quantum numbers there is no obvious reason why this should be the case. Despite this the cancellation of the interior quantum numbers by those at boundaries or light-like causal determinants could occur and would conform with the effective 2-dimensionality stating that quantum states are characterized by partonic boundary states associated with causal determinants. This could be also seen as a holographic duality of interior and boundary degrees of freedom [K11].

2.2 Can One Regard # *Resp.* $\#_B$ Contacts As Particles *Resp.* String Like Objects?

#-contacts have obvious particle like aspects identifiable as either partons or parton pairs. $\#_B$ contacts in turn behave like string like objects. Using the terminology of M-theory, $\#_B$ contacts connecting the boundaries of space-time sheets could be also seen as string like objects connecting two branes. Again the ends holes at the ends of $\#_B$ contacts carry well defined gauge charges.

2.2.1 # contacts as particles and $\#_B$ contacts as string like objects?

The fact that # contacts correspond to parton pairs raises the hope that it is possible to apply p-adic thermodynamics to calculate the masses of # contact and perhaps even the masses of the partons. If this the case, one has an order of magnitude estimate for the first order contribution to the mass of the parton as $m \sim 1/L(p_i)$, $i = 1, 2$. It can of course happen that the first order contribution vanishes: in this case an additional factor $1/\sqrt{p_i}$ appears in the estimate and makes the mass extremely small.

For # contacts connecting space-time sheets with opposite time orientations the vanishing of the net four-momentum requires $p_1 = p_2$. According to the number theoretic considerations below it is possible to assign several p-adic primes to a given space-time sheet and the largest among them, call it p_{max}, determines the p-adic mass scale. The milder condition is that p_{max} is same for the two space-time sheets.

There are some motivations for the working hypothesis that # contacts and the ends of $\#_B$ contacts feeding the gauge fluxes to the lower condensate levels or vice versa tend to be located near the boundaries of space-time sheets. For gauge charges which are not screened by vacuum charges (em and color charges) the embedding of the gauge fields created by the interior gauge charges becomes impossible near the boundaries and the only possible manner to satisfy boundary conditions is that gauge fluxes flow to the larger space-time sheet and space-time surface becomes a vacuum extremal of the Kähler action near the boundary.

For gauge bosons the density of boundary $\#_B$ contacts should be very small in length scales, where matter is essentially neutral. For gravitational $\#_B$ contacts the situation is different. One might well argue that there is some upper bound for the gravitational flux associated with single # or $\#_B$ contact (or equivalently the gravitational mass associated with causal horizon) given by Planck mass or CP_2 mass so that the number of gravitational contacts is proportional to the mass of the system.

The TGD based explanation for Podkletnov effect [H2] is based on the assumption that magnetically charged # contacts are carries of gravitational flux equal to Planck mass and predicts effect with correct order of magnitude. The model generalizes also to the case of $\#_B$ contacts. The lower bound for the gravitational flux quantum must be rather small: the mass $1/L(p)$ determined by the p-adic prime associated with the larger space-time sheet is a first guess for the unit of flux.

2.2.2 Could # and $\#_B$ contacts form Bose-Einstein condensates?

The description as # contact as a parton pair suggests that it is possible to assign to # contacts inertial mass, say of order $1/L(p)$, they should be describable using d'Alembert type equation for a scalar field. # contacts couple dynamically to the geometry of the space-time since the induced metric defines the d'Alembertian. There is a mass gap and hence # contacts could form a Bose-Einstein (BE) condensate to the ground state. If # contacts are located near the boundary of the

space-time surface, the d'Alembert equation would be 3-dimensional. One can also ask whether # contacts define a particular form of dark matter having only gravitational interactions with the ordinary matter.

Also the probability amplitudes for the positions of the ends of $\#_B$ contacts located at the boundary of the space-time sheet could be described using an order parameter satisfying d'Alembert equation with some mass parameter and whether the notion of Bose-Einstein condensate makes sense also now. The model for atomic nucleus assigns to the ends of the $\#_B$ contact realized as a color magnetic flux tube quark and anti-quark with mass scale given by $k = 127$ (MeV scale) [K12].

This inspires the question whether # and $\#_B$ contacts could be essential for understanding bio-systems as macroscopic quantum systems [K5]. The BE condensate associated with the # contacts behaves in many respects like super conductor: for instance, the concept of Josephson junction generalizes. As a matter fact, it seems that $\#_B$ contacts, join along boundaries, or magnetic flux tubes could indeed be a key element of not only living matter but even nuclear matter and condensed matter in TGD Universe. One application of the concept is the TGD based explanation [K16] of Comorosan1 effect [I2, I1] in terms of # contact Josephson currents appearing at molecular level.

2.2.3 The transfer of fields between space-time sheets and # and $\#_B$ contacts

The penetration of the external electric and magnetic fields from external world to subsystem (from larger space-time sheet to a smaller one) and vice versa must take place via the creation and re-arrangement of the # and $\#_B$ contacts and also by the generation of # and $\#_B$ contact currents. The unique coupling of the wormhole BE condensate to the geometry of the boundary of the space-time sheet together with the classical electromagnetic interaction between wormholes and electrons implies coupling between electrons and the shape and size of the 3-surface. This coupling might make it possible to understand how bio-systems are able to control their size and shape.

2.2.4 Exotic effects related to the many-sheeted space-time

The hopping of electrons (most probably unpaired valence electrons) from the atomic space-time sheet to non-atomic space-time sheets might be energetically favorable under some circumstances and would lead to the formation of "exotic atoms" and effective electronic alchemy since the chemical properties of the atom are presumably determined by the electronic properties of the atomic space-time sheet [K7]. The "exotic" electrons on non-atomic space-time sheets provide an ideal mechanism for energy and charge transfer since dissipative effects are small and even the temperature at these space-time sheets might be much smaller than the temperature at the atomic space-time sheet. In this respect bio-systems are especially interesting.

The interaction of the exotic electrons with the wormhole BE condensate takes place via the classical electromagnetic interaction generating excitations of the # contact BE condensate. The mechanism is completely analogous to the ordinary mechanism of super conductivity in which electromagnetic interaction of electrons with nuclei excites phonons. Since the gap energy is of order $1/L(p)$ characterizing the size of the p-adic space-time sheet, one can consider the possibility of high temperature super conductivity.

One can even consider the possibility that the presence of electrons on "wrong" space-time sheets makes if favorable for some atomic nuclei to feed their electromagnetic charges to non-atomic space-time sheets. This would in principle make possible Trojan horse mechanism of cold nuclear fusion since two nuclei feeding their electromagnetic gauge fluxes on different space-time sheets do not see the Coulomb wall [K12].

Also ions can drop to larger space-time sheets. In [K3, K4] a model of ionic high T_c super conductivity explaining certain peculiar effects of the em radiation on living matter is considered. These effects actually provide support for the view that living systems are macroscopic quantum systems.

2.3 Number Theoretical Considerations

Number theoretical considerations allow to develop more quantitative vision about the how p-adic length scale hypothesis relates to the ideas just described.

2.3.1 How to define the notion of elementary particle?

p-Adic length scale hierarchy forces to reconsider carefully also the notion of elementary particle. p-Adic mass calculations led to the idea that particle can be characterized uniquely by single p-adic prime characterizing its mass squared. It however turned out that the situation is probably not so simple.

The work with modelling dark matter suggests that particle could be characterized by a collection of p-adic primes to which one can assign weak, color, em, gravitational interactions, and possibly also other interactions. It would also seem that only the space-time sheets containing common primes in this collection can interact. This leads to the notions of relative and partial darkness. An entire hierarchy of weak and color physics such that weak bosons and gluons of given physics are characterized by a given p-adic prime p and also the fermions of this physics contain space-time sheet characterized by same p-adic prime, say M_{89} as in case of weak interactions. In this picture the decay widths of weak bosons do not pose limitations on the number of light particles if weak interactions for them are characterized by p-adic prime $p \neq M_{89}$. Same applies to color interactions.

The p-adic prime characterizing the mass of the particle would perhaps correspond to the largest p-adic prime associated with the particle. Graviton which corresponds to infinitely long ranged interactions, could correspond to the same p-adic prime or collection of them common to all particles. This might apply also to photons. Infinite range might mean that the flux tubes mediating these interactions can be arbitrarily long but their transversal sizes are characterized by the p-adic length scale in question.

The natural question is what this collection of p-adic primes characterizing particle means? The hint about the correct answer comes from the number theoretical vision, which suggests that at fundamental level the branching of boundary components to two or more components, completely analogous to the branching of line in Feynman diagram, defines vertices [K6, K13].

1. If space-time sheets correspond holographically to multi-p p-adic topology such that largest p determines the mass scale, the description of particle reactions in terms of branchings indeed makes sense. This picture allows also to understand the existence of different scaled up copies of QCD and weak physics. Multi-p p-adicity could number theoretically correspond to q-adic topology for $q = m/n$ a rational number consistent with p-adic topologies associated with prime factors of m and n ($1/p$-adic topology is homeomorphic with p-adic topology).

2. One could also imagine that different p-adic primes in the collection correspond to different space-time sheets condensed at a larger space-time sheet or boundary components of a given space-time sheet. If the boundary topologies for gauge bosons are completely mixed, as the model of hadrons forces to conclude, this picture is consistent with the topological explanation of the family replication phenomenon and the fact that only charged weak currents involve mixing of quark families. The problem is how to understand the existence of different copies of say QCD. The second difficult question is why the branching leads always to an emission of gauge boson characterized by a particular p-adic prime, say M_{89}, if this p-adic prime does not somehow characterize also the particle itself.

2.3.2 What effective p-adic topology really means?

The need to characterize elementary particle p-adically leads to the question what p-adic effective topology really means. p-Adic mass calculations leave actually a lot of room concerning the answer to this question.

1. The naïvest option is that each space-time sheet corresponds to single p-adic prime. A more general possibility is that the boundary components of space-time sheet correspond to different p-adic primes. This view is not favored by the view that each particle corresponds to a collection of p-adic primes each characterizing one particular interaction that the particle in question participates.

2. A more abstract possibility is that a given space-time sheet or boundary component can correspond to several p-adic primes. Indeed, a power series in powers of given integer n

gives rise to a well-defined power series with respect to all prime factors of n and effective multi-p-adicity could emerge at the level of field equations in this manner.

One could say that space-time sheet or boundary component corresponds to several p-adic primes through its effective p-adic topology in a hologram like manner. This option is the most flexible one as far as physical interpretation is considered. It is also supported by the number theoretical considerations predicting the value of gravitational coupling constant [K13].

An attractive hypothesis is that only space-time sheets characterized by integers n_i having common prime factors can be connected by join along boundaries bonds and can interact by particle exchanges and that each prime p in the decomposition corresponds to a particular interaction mediated by an elementary boson characterized by this prime.

2.3.3 Do infinite primes code for q-adic effective space-time topologies?

Besides the hierarchy of space-time sheets, TGD predicts, or at least suggests, several hierarchies such as the hierarchy of infinite primes [K13], hierarchy of Jones inclusions [K15], hierarchy of dark matters with increasing values of $\hbar$ [K8, K7], the hierarchy of extensions of given p-adic number field, and the hierarchy of selves and quantum jumps with increasing duration with respect to geometric time. There are good reasons to expect that these hierarchies are closely related.

1. Some facts about infinite primes

The hierarchy of infinite primes can be interpreted in terms of an infinite hierarchy of second quantized super-symmetric arithmetic quantum field theories allowing a generalization to quaternionic or perhaps even octonionic context [K13]. Infinite primes, integers, and rationals have decomposition to primes of lower level.

Infinite prime has fermionic and bosonic parts having no common primes. Fermionic part is finite and corresponds to an integer containing and bosonic part is an integer multiplying the product of all primes with fermionic prime divided away. The infinite prime at the first level of hierarchy corresponds in a well defined sense a rational number $q = m/n$ defined by bosonic and fermionic integers m and n having no common prime factors.

2. Do infinite primes code for effective q-adic space-time topologies?

The most obvious question concerns the space-time interpretation of this rational number. Also the question arises about the possible relation with the integers characterizing space-time sheets having interpretation in terms of multi-p-adicity. On can assign to any rational number $q = m/n$ so called q-adic topology. This topology is not consistent with number field property like p-adic topologies. Hence the rational number q assignable to infinite prime could correspond to an effective q-adic topology.

If this interpretation is correct, arithmetic fermion and boson numbers could be coded into effective q-adic topology of the space-time sheets characterizing the non-determinism of Kähler action in the relevant length scale range. For instance, the power series of $q > 1$ in positive powers with integer coefficients in the range $[0, q)$ define q-adically converging series, which also converges with respect to the prime factors of m and can be regarded as a p-adic power series. The power series of q in negative powers define in similar converging series with respect to the prime factors of n.

I have proposed earlier that the integers defining infinite rationals and thus also the integers m and n characterizing finite rational could correspond at space-time level to particles with positive *resp.* negative time orientation with positive *resp.* negative energies. Phase conjugate laser beams would represent one example of negative energy states. With this interpretation super-symmetry exchanging the roles of m and n and thus the role of fermionic and bosonic lower level primes would correspond to a time reversal.

1. The first interpretation is that there is single q-adic space-time sheet and that positive and negative energy states correspond to primes associated with m and n respectively. Positive (negative) energy space-time sheets would thus correspond to p-adicity ($1/p$-adicity) for the field modes describing the states.

2. Second interpretation is that particle (in extremely general sense that entire universe can be regarded as a particle) corresponds to a pair of positive and negative energy space-time sheets labelled by m and n characterizing the p-adic topologies consistent with $m-$ and n-adicities. This looks natural since Universe has necessary vanishing net quantum numbers. Unless one allows the non-uniqueness due to $m/n = mr/nr$, positive and negative energy space-time sheets can be connected only by # contacts so that positive and negative energy space-time sheets cannot interact via the formation of $\#_B$ contacts and would be therefore dark matter with respect to each other.

Positive energy particles and negative energy antiparticles would also have different mass scales. If the rate for the creation of # contacts and their CP conjugates are slightly different, say due to the presence of electric components of gauge fields, matter antimatter asymmetry could be generated primordially.

These interpretations generalize to higher levels of the hierarchy. There is a homomorphism from infinite rationals to finite rationals. One can assign to a product of infinite primes the product of the corresponding rationals at the lower level and to a sum of products of infinite primes the sum of the corresponding rationals at the lower level and continue the process until one ends up with a finite rational. Same applies to infinite rationals. The resulting rational $q = m/n$ is finite and defines q-adic effective topology, which is consistent with all the effective p-adic topologies corresponding to the primes appearing in factorizations of m and n. This homomorphism is of course not 1-1.

If this picture is correct, effective p-adic topologies would appear at all levels but would be dictated by the infinite-p p-adic topology which itself could refine infinite-P p-adic topology [K13] coding information too subtle to be caught by ordinary physical measurements.

Obviously, one could assign to each elementary particle infinite prime, integer, or even rational to this a rational number $q = m/n$. q would associate with the particle q-adic topology consistent with a collection of p-adic topologies corresponding to the prime factors of m and n and characterizing the interactions that the particle can participate directly. In a very precise sense particles would represent both infinite and finite numbers.

2.3.4 Under what conditions space-time sheets can be connected by $\#_B$ contact?

Assume that particles are characterized by a p-adic prime determining it mass scale plus p-adic primes characterizing the gauge bosons to which they couple and assume that $\#_B$ contacts mediate gauge interactions. The question is what kind of space-time sheets can be connected by $\#_B$ contacts.

1. The first working hypothesis that comes in mind is that the p-adic primes associated with the two space-time sheets connected by $\#_B$ contact must be identical. This would require that particle is many-sheeted structure with no other than gravitational interactions between various sheets. The problem of the multi-sheeted option is that the characterization of events like electron-positron annihilation to a weak boson looks rather clumsy.

2. If the notion of multi-p p-adicity is accepted, space-time sheets are characterized by integers and the largest prime dividing the integer might characterize the mass of the particle. In this case a common prime factor p for the integers characterizing the two space-time sheets could be enough for the possibility of $\#_B$ contact and this contact would be characterized by this prime. If no common prime factors exist, only # contacts could connect the space-time sheets. This option conforms with the number theoretical vision. This option would predict that the transition to large $\hbar$ phase occurs simultaneously for all interactions.

2.4 Physically Interesting P-Adic Length Scales In Condensed Matter Systems

Table 1 lists the p-adic length scales L_p. p near prime power of 2, which might be interesting as far as condensed matter is considered. It must be emphasized that the definition of length scale is bound to contain some unknown numerical factor and numbers should not be taken too literally.

k	127	131	137	139	149
L_p/m	$2.04E-12$	$8.19E-12$	$6.53E-11$	$1.31E-10$	$4.18E-9$
k	151	157	163	167	173
L_p/m	$8.33E-9$	$6.69E-8$	$5.34E-7$	$2.13E-6$	$1.71E-5$
k	179	181	191	193	
L_p/m	$1.37E-4$	$2.74E-4$	$8.85E-3$	$1.75E-2$	

Table 1: p-Adic length scales $L_p = 2^{k-127}L_{127}$, $p \simeq 2^k$, $L_{127} \equiv \frac{\pi\sqrt{5+Y}}{m_e}$, $Y = .0317$, k prime, possibly relevant to condensed matter physics.

Notice that the length scales $L(137)$ and $L(139)$ are quite near to the typical atomic length scale and this suggests that the lattice structures of solid state physics might be understood in terms of structures formed by gluing together p-adic cubes with size $L(137)$ by join along boundaries bonds/flux tubes.

3 Hydrodynamical And Thermodynamical Hierarchies

The existence of p-adic length scale hierarchy suggests a new approach to hydrodynamics. There is hydrodynamic flow associated with each condensate level h. The particles at level are condensate blocks of the previous level having typically size $L_{upper}(k)$ larger than $L(k)$ and hydrodynamic approximation fails at this length scale. It will be found that the phenomenon of sono-luminescence can be interpreted as evidence for the hydrodynamical hierarchy. The masses of these particles are just the masses of condensate blocks. The energy dissipation at given level takes place via the collisions of condensate blocks and one can get an order of magnitude estimate for the viscosity $\nu(k)$ and other transport coefficients at level k using kinetic gas theory for condensate blocks.

There must exist also energy transfer mechanism transporting energy and angular momentum to higher condensate levels and eventually to atomic condensation level and this mechanism should be work at length scales $L < L_{upper}(k)$, at which hydrodynamic approximation fails at level k. The mechanism to be proposed is completely analogous with the penetration of magnetic fields into super conductor and should be possible in sufficiently long length scales: the convective zone of Sun provides a possible realization of the mechanism. The hierarchy means quite rich possibilities for flows: the fluid need not be in same phase at all levels, the temperatures (temperature distributions) at different levels need not be identical. The character of the flow need not be same at different levels (turbulent/ non-turbulent, rotational/irrotational, etc).

3.1 Dissipation By The Collisions Of Condensate Blocks

Collisions of condensate blocks at level k provide one possible dissipation mechanism and just as in molecular case the mechanism can be characterized viscosity coefficient. One can generalize kinetic gas theory estimate for the kinetic viscosity at level k in straightforward manner.

$$\begin{aligned}
\nu(k) &= \lambda(k)\beta \ , \\
\lambda(k) &= \frac{1}{N(block)\sigma(k)} \ , \\
\sigma(k) &\sim 4\pi L^2_{upper}(k) \ , \\
N(block) &\sim \frac{1}{L_{upper}(k)^3} \ , \\
\beta &\sim \beta_{th} \sim \sqrt{\frac{T(k)}{M(block)}} \ , \\
M(block) &\sim N(nucleus) M L^3_{upper}(k) \ ,
\end{aligned} \tag{3.1}$$

where the average velocity β is replaced with thermal velocity to obtain order of magnitude estimate. More explicitly,

$$\begin{aligned} \nu(k) &= \sqrt{\frac{L(139)}{L_{upper}(k)}}\nu(139) \ , \\ \nu(139) &= \frac{1}{4\pi N(nucleus,139)}\sqrt{\frac{T}{M}}L(139) \ . \end{aligned} \tag{3.2}$$

The order of magnitude $\nu(139)$ is roughly the same as the order of magnitude for ordinary viscosity at room temperatures determined by the size of the atom. From formula it is clear that $\nu(k)$ scales as $\sqrt{1/L(k)}$. This means that the importance of the collisions of the condensate blocks as dissipation mechanism decreases rapidly in long p-adic length scales. This does not necessarily mean the absence of dissipation since mechanisms of energy transfer between condensate levels must exist. Reynolds number criterion implies that the flow is in sufficiently long p-adic length scales always turbulent.

The collisions of the condensate block need not be elastic and the collision at level k in general involves simultaneous collisions at levels $k_1 < k$ up to atomic condensate levels so that it leads to energy dissipation at all condensate levels $k_1 \geq k$. An interesting challenge is the description of shock waves in this picture. A shock wave at level k corresponds to "traffic jam" in shock front involving the collisions of the condensate blocks at level k. This in turn is expected to lead to shock waves propagating inside condensate blocks at level $k_{prev} < k$ and so on. Shock wave hierarchy ends up to the atomic condensate level $k = 131$.

3.2 Energy Transfer Between Different Condensate Levels In Turbulent Flow

The model for the generation of hydrodynamic turbulence is based on the idea that hydrodynamic vortices correspond to topological field quanta, that is cylindrical 3-surfaces with finite radius carrying Kähler electric and magnetic fields. The completely new feature is the presence of ordinary or Z^0 magnetic fields determining the size of the hydrodynamic vortices. Even the Reynolds number criterion could be formulated in terms of these fields. The naïve expectation would be that the vortices could be characterized as either em or Z^0 vortices. This is actually not the case since induced gauge field concept implies that em fields are accompanied by Z^0 fields and vice versa for extremals of Kähler action. The study of the embeddings for Kähler electric and magnetic fields led to the conclusion that vorticities are specified by two frequency type parameters ω_i and by two integers n_i related to the space-time dependence of the phases of the two complex CP_2 coordinates plus and integer m: the vortices with different value of fractal quantum number m were related by a power of a discrete scaling transformation to each other. The decay of vortices to smaller vortices leading to a cascade was suggested to be the basic mechanism for the generation of turbulence. The model led to estimates for Reynolds number for the transition to turbulence in channel flow and for the exponent Δ appearing in the Fourier transform $T(k) \propto k^{\Delta}$ of the kinetic energy density of the flow. In recent context the model for the decay of vortices can be regarded as a kinetic model for the vortices of level k appearing as particles at the level k_{next}.

p-Adic picture of condensed matter suggests a considerable generalization of this model. Of course, a lot of work is needed to construct a detailed quantitative model but some general features of the model are evident.

1. The proposed cascade mechanism as such works at single condensate level for vortices having size larger than $L_{upper}(k)$: below this length scale the hydrodynamic approximation fails. The lower bound for the vortex size was assumed to be some scale not much above atomic size so that description might apply as such at condensate level $k = k_Z$.

2. The idea already due to Kolmogorov [B2] is that the generation of turbulence involves the interaction between many length scales: in turbulent situation constant power ϵ is fed to the system of size l and the rate of the energy flow between any subsequent levels in the hierarchy

of length scales is constant and dissipation becomes important at the highest levels of the hierarchy, which correspond to the shortest length scales $L_0 \sim l/Re^{3/4}$ related by to the length scale of the entire flow. This idea leads directly to important dimensional estimates making possible to deduce the form of the velocity correlation function in length scales at which dissipation is not important. It is perhaps worth of recalling that the turbulence model gives slightly different value for the exponent Δ associated with the energy density.

This interaction between different scales corresponds to the decay of vortices to smaller vortices with scaled down values of the vorticity and critical radius: this picture probably still applies at single condensate level down to the vortex radii of order $L_{upper}(k)$, where the hydrodynamical approximation fails. If the size of the block is much larger than the size λ_0 of eddies important for energy dissipation (having Reynolds number of order one) collisions of the condensate blocks at level k cannot take care of energy dissipation. Using the standard order of magnitude estimate for λ_0 [B2] the criterion for dissipation via collisions to be possible reads as

$$\begin{aligned} L_{upper}(k) &< \lambda_0(k) \ , \\ \lambda_0(k) &= \frac{l}{Re^{3/4}(k)} = (\frac{L(139)}{L(k)})^{3/8}\lambda_0(139) \ . \end{aligned} \tag{3.3}$$

$\lambda_0(139)$ is roughly of same order of magnitude as the estimate based on molecular viscosity and it is clear that in long p-adic length scales the condition cannot be met. One has $\lambda_0(k) \sim 2^{-(k-139)/2}10^{-3}l$ (assuming for definiteness $R \sim 10^4$ in turbulent flow) and L is bound to be smaller than $L_{upper}(k)$ unless l is very large as compared with $L(k)$. Since constant energy dissipation is taking place there must exist some mechanism of energy and angular momentum transfer between condensate levels and this mechanism is expected to be at work below the length scales below, at which hydrodynamic approximation works.

The structure of the topological condensate suggests much more general realization for the idea about interacting length scales: besides vortices related by powers of discrete scaling transformation also different levels k of topological condensate correspond to the levels of the hierarchy. The external source of energy and angular momentum is at some level $k >> 131$ (a concrete example is provided by channel flow) and the flow of energy occurs first from large to smaller eddies at level k in accordance with the standard picture and continues to the higher level k_{prev} via some energy transfer mechanism and repeats itself at level k_{prev}.

If condensate has hierarchical structure the flow occurs in good approximation only between two subsequent condensate levels. The previous work suggests that the mechanism is based on generation of vortices at level k_{cr} and that ordinary and Z^0 magnetic fields might play key role in the mechanism. The length scale $L(k_Z)$ means clearly a borderline in the generation of turbulence. For levels with $k > k_Z$ the electro-weak gauge fields are of Z^0 and em type and there is no motion in atomic length scales. At level $k = k_Z$ the motion is transferred to atomic level since nuclei feed their Z^0 charges directly at $k = k_Z$ level. At levels $k > k_Z$ ordinary magnetic vortices should take the role of Z^0 and em vortices. $k = k_Z$ level is special in the sense that the entire fluid motion at length scales $k > k_Z$ is seen in the flow pattern of Z^0 # throats at this level. It should be also noticed that p-adic quantized version of hydrodynamics (whatever it might mean!) is in principle involved at level $k = k_Z$.

p-Adic TGD suggests a detailed mechanisms for the flow of energy, angular momentum and magnetic flux from level k to level k_{prev}.

1. In the simplified description there are two kind of lumps of rotational energy at level k. The rigid body rotation of the condensate blocks of level k_{prev} condensed on level k and the vortices formed by the condensate blocks, each block rotating according to the law $\beta(\rho) = K/\rho$, where K is vorticity (essentially the total angular momentum) and ρ the distance from the vortex axis. The basic energy transfer process must take place at the level of single condensate block of size not very much larger than $L(k)$ produced as the end result of the cascade process. The block is in rigid body rotation and the destruction of the super fluidity by rigid body rotation of the vessel containing super fluid suggests the mechanism. When

the approximately constant magnetic field created by vortex motion at level k is sufficiently strong at the position of the block it penetrates to the level k_{prev}.

2. According to the previous proposal this mechanism is following. For $\Omega < \Omega_{crit}$ the Z^0 and/or em magnetic fields created by the rotation of the # throats on the boundary of the block at level k are those of an extended magnetic dipole: inside the vortex the field lines run in the direction of vortex. For $\Omega = \Omega_{cr}$ something very peculiar happens: the magnetic field created by the rotational flow penetrates to the higher condensate level via # contacts formed at the upper and lower end of the vortex, which behave as magnetic dipoles at levels k and k_{prev}. This means that the magnetic flux runs from the level k to k_{prev} and vice versa at the opposite ends of the vortex and the conservation of magnetic flux implies that average magnetic fluxes are identical on the two levels. The field inside the vortex cylinder disappears at level k and only the field lines of the return flux outside the vortex are preserved. Since magnetic flux and angular momentum are closely related this requires that the rotating block is set in rigid body motion with angular momentum opposite to the angular momentum of the entire block in vortex motion. There blocks in vortex would rotate in opposite direction as compared to the vortex and angular momentum is indeed transferred from level k to k_{prev}.

3. The analogy with super conduticity/super fluidity suggests that the process cannot take place for too small value of magnetic field/rotational velocity at level k. Since the vorticity can be written as $K = \beta\rho$ the condition $K > K_{cr}$ is analogous (but not equivalent) with the Reynolds number criterion $ud > Re_{cr}\nu$. The criterion $K > K_{cr}$ translates into the condition $B > B_{cr}$. The physical content of the condition is probably the following. In the absence of the vortices liquid at level k_{prev} tends to form large join along boundaries/flux tube blocks: for dense liquids only very few large join along boundaries/flux tube block are present whereas for the gases there are only few flux tubes present. The formation of vortices splits flux tubes at the boundaries of the vortices and some energy $E_{join}(k)$ must be taken from the flow to split single flux tubes if present.

4. The criterion for the penetration of magnetic field must be local in the sense that only the energetics of a single join along boundaries bond/flux tube is involved. A natural guess is that the magnetic energy contained in the volume of the bond is larger than the binding energy of the bond: $E_B > E(join)$. Since B is proportional to the vorticity K, the criterion gives critical vorticity K_{cr}. The dependence of $E_B \propto b/L^3(k)$ with b integer implies that the dependence of E_B and $E(join)$ on $L(k)$ is same and K_{cr} does not depend on condensate level. In this case $K_{cr} < K_{Re} \equiv ud = Re \cdot \nu$ holds true unless b is very large integer of order 10^{39} and criterion is identically satisfied for turbulent flow. If b is rational number with small denominator, one has effectively $E_{join} = b/L(k)$ for the real counterpart of the energy and one obtains $K_{cr} \propto L(k)$, which is probably the correct alternative. In sufficiently long length scales (perhaps all physically interesting length scales) one has $K_{cr} > K_{Re} \equiv ud = Re \cdot \nu$, which implies a lower bound for the size of the vortices of the turbulent flow in the range $K_{Re} < K < K_{cr}$. This means that for liquids the energy transfer mechanism comes into play for very large Reynolds numbers only and should manifest itself in long (perhaps astrophysical) length scales only. For gases the situation is different since the criterion makes sense only provided the density of the join along boundaries bonds is large (incompressible flow) and in ordinary gas flow the criterion is not needed.

5. The disappearance of the vortices at the highest condensation levels can be regarded as resulting from the annihilation of magnetic monopoles associated with the upper and lower ends of the vortices. One possibility is self destruction, when the mopoles and upper and lower ends annihilate. Second possibility is the annihilation of two different vortices. At lower level the process implies the recombination of the magnetic field lines at positions of monopoles.

6. A possible astrophysical example of the proposed energy transfer process is provided by the convective zone of the Sun, where the presence of the magneticized vortex like structures of all sizes is directly visible. Only observational limitations set lower bound for the radii of the vortices. The ends of the magnetic dipoles are visible and also the recombination of field

lines of magnetic fields (this can be regarded as annihilation of magnetic monopoles!) occurs frequently [E2].

7. The assumption that the flow consists of vortices carrying almost constant magnetic fields, is not necessary. What is important is the behavior of the magnetic field created by the main flow in the region of single condensate block participating in the flow. If the magnetic field does not vary much in the region of the block, the penetration can take place via the same mechanism into the block. A possible test for the proposed scenario is the flow in the external magnetic field at level $k < k_Z$: for some critical value of field (probably rather high) the flow should become turbulent. One can also consider creating external Z^0 magnetic fields in the interior of, say rotating cylinder, and finding whether they affect the properties of the non-turbulent flow inside the cylinder.

3.3 The Magnetic Fields Associated With Vortex And Rigid Body Flows

The magnetic field associated with vortex flow $\beta = K/\rho$ (ρ is the distance from the axis of vortex) is given by

$$\begin{aligned} B_C &= A_C K ln(\frac{\rho}{\rho_0}),\ C = em, Z\ , \\ A_C &= \frac{g_C q_C}{\sqrt{\epsilon_C(k)}} n(nucleus)\ , \\ Q_Z &= (A-Z)Q_Z(n) \quad Q_{em} = Z\ , \end{aligned} \tag{3.4}$$

where ρ_0 is some finite radius at which the flow ceases to be vortex flow and is expected to change to rigid body flow (single condensate block rotates as rigid body). ϵ_C will be assumed to satisfy the simple scaling law $\epsilon_C(k) \propto L(k)^6$. The field is in good approximation constant in region of vortex so that critical field condition leading to the penetration of the field to higher level occurs almost simultaneously in vortex but proceeds from boundary to interior.

The magnetic field associated with rigid body flow $\beta = \Omega\rho$ is given by

$$B_C = A_C \Omega \frac{\rho^2}{2}\ , \tag{3.5}$$

where the parameter A_C defined in previous formula. At critical value of vortex magnetic field condensate blocks rotating in vortex flow like rigid bodies begin to rotate counterclockwise with regard to the vortex flow and the angular rotation velocity is such that

i) the magnetic fluxes created by rigid body flow and vortex flow cancel each other or

ii) angular momentum in the region of condensate block is transferred to higher condensate level.

Denoting the radius of a rigidly rotating block in the vortex flow by ρ_{rig} and by ρ_1 the distance of the block from the axis of vortex flow one obtains for the value of the angular velocity parameter Ω

$$\begin{aligned} \Omega &\simeq \frac{2K}{\rho_{rig}^2} X\ , \\ X &= ln(\rho_1/rho_0)\ . \end{aligned} \tag{3.6}$$

An almost identical condition

$$\Omega \simeq \frac{2K}{\rho_{rig}^2}\ , \tag{3.7}$$

is obtained if one requires that entire angular momentum of the rigidly rotating block in vortex flow is transferred to higher condensate level so that the two models are equivalent with logarithmic accuracy.

3.4 Criticality Condition

Consider next the criticality condition for vortex magnetic field or equivalently vorticity $K \sim ud$ to derive the analog of Reynolds number criterion $ud > Re \cdot \nu$ for single vortex. The condition states that magnetic field energy in the volume of join along boundaries bond/flux tubes is larger than flux tubeing energy E_{join}.

$$E_B(bond) \quad > \quad E_{join} \ , \tag{3.8}$$

to derive more quantitative criterion one must make some additional assumptions. The volume of flux tube at level k is assumed to be of order $L^3(k)$ since bond should consist of few p-adic cubes glued together along their walls. E_{join} is of form $bp^{3/2}$ p-adically. If b is integer the real counterpart of the energy behaves as $1/L(k)^3$ and if b is rational number with small denominator the real counterpart of energy behaves as $a/L(k)$, $a < 1$.

The following argument suggests that b must be a genuine rational number. The radius ρ_{cr} of the condensate block determined from the imbeddability requirement of the magnetic field as induced gauge field must be equal to the radius $L_{upper}(k) \propto L(k)$ of the block determined by the stability against topological evaporation. This is possible only provided $\rho_{cr} \propto L(k)$ holds true. It will be later found that the dependence of ρ_{cr} on p-adic length scales is as follows

$$\rho_{cr} \quad \propto \quad \frac{\epsilon_C^{1/4}}{K^{1/2}} \propto \frac{L(k)^{3/2}}{b^{1/2}} \ . \tag{3.9}$$

For integer b this gives $\rho_{cr} \propto L(k)^{3/2}$ so that the critical radius is larger than $L_{upper}(k)$ at large length scales. If b is rational number one indeed has $\rho_{cr} \propto L(k)$ and ρ_{cr}. In this case both K_{cr} and ρ_{cr} are proportional to $L(k)$ as suggested by fractality.

If Z^0 magnetic fields dominate at levels $k > k_Z$ levels the condition reduces for $E_{join} = b/L(k)$ to the form

$$\begin{aligned} K &> K_{cr}(k) \ , \\ K_{cr}(Z,k) &= K_Z L(k) \ , \\ K_Z &= b^{1/2} 2^{-41} \frac{\sqrt{\epsilon_Z(k_Z)}}{g_Z(A-Z)} B \ , \\ B &= \frac{\sqrt{2}}{N(nucleus,139)} \frac{1}{ln(\frac{\rho_1}{\rho_0})} \ , \end{aligned} \tag{3.10}$$

which gives $K_{cr}(k) \sim \sqrt{b} \cdot 5 \cdot 10^{-2} L(k)$ for $\epsilon_Z(k_Z) \sim 10^{24}$. At condensate levels $k < k_Z$, where ordinary magnetic fields are in question, the condition reads

$$\begin{aligned} K_{cr}(em,k) &= K_{em} L(k) \ , \\ K_{em} &= b^{1/2} 2^{12} \frac{\sqrt{\epsilon_Z(131)}}{Ze} B L(k) \ . \end{aligned} \tag{3.11}$$

B is given by the previous formula. This gives $K_{cr}(k) \sim \sqrt{b} 10^4 L(k)$ ($b < 1$). The value of $K_{Re} = Re \cdot \nu$ is of order 10^{-10} m for typical values $Re = 10^4$ and $\nu \sim 10^{-14}$ m so that K_{cr} is always larger than K_{Re} unless b is very small. This means that below the length scale $L(k_Z)$ the proposed energy transfer mechanism comes into play at very large Reynolds numbers of order

$$Re \quad \sim \quad \frac{K_{cr}(em,k)}{\nu} \sim 10^5 b^{1/2} \frac{L(k)}{L(107)} \ , \tag{3.12}$$

whereas for gas phase the situation is different. When $L_{upper}(k)$ is much larger than the size $L_0 \sim l/Re^{3/4}$ for dissipative eddies with $Re \sim 1$ and $K < K_{cr}$ so that the collisions of the join along boundaries blocks nor the proposed energy transfer mechanism cannot take care of the dissipation and some other mechanisms of dissipation must be active: one possibility is heating leading to the splitting of the flux tubes.

The assumption that the mechanism is at work in the convective zone of Sun gives information on the value value of the parameter b. Assuming $\beta \sim 10^{-5}$ and $L_{upper}(k) \sim 10^7$ m one obtains from $K \sim L_{upper}\beta \sim 10^2$ m. The criterion gives $b^{1/2}L(k) \leq 2 \cdot 10^2$ m. An estimate for b is obtained using the relation $L_{upper}(k) \leq AL(k)$, $A \sim 10^2$: for $L_{upper} \sim 10^2 L(k)$ one obtains $b \sim 4 \cdot 10^{-6}$. $L(k)$ and therefore b can be estimated if one has some idea about the value of B_Z: this together with estimate for K gives grasp on the value of $\epsilon_Z(k)$ and scaling law gives estimate for $L(k)$.

The condition implies that typical angular velocities Ω for rigid body rotation behave as $\Omega(k) \propto 1/L(k)$ and that average rotation velocities $\beta(k)$ are identical for all condensate levels. This implies that the frequency spectrum associated with the flow is superposition of form

$$F_{tot}(\omega) \quad = \quad \sum_{k\ prime} a_k F(\omega \frac{L(k_0)}{L(k)}) \ , \tag{3.13}$$

and the general form of the spectrum in principle provides a test for p-adic length scale hypothesis. $\beta(k) = constant$ suggests that spatial correlation function for velocity is constant and its Fourier spectrum corresponds to white noise spectrum.

For completeness it is useful to give the values of K_{cr} also for the $E_{join} = bL_0^2/L^3(k)$ ($L_0 \sim 10^4\sqrt{G}$ being the fundamental p-adic length scale) case.

$$K_{cr}(C) \quad = \quad k_C L_0 \ . \tag{3.14}$$

The only difference with respect to previous formulas is the replacement $L(k) \to L_0$. For small values of b the condition is automatically satisfied for reasonable values of K and the sizes of vortices should have no lower bound above atomic length scales: this is not in accordance with the estimate $\lambda_0 \sim l/Re^{3/4}$ of Kolmogorov theory.

3.5 Sono-Luminescence, Z^0 Plasma Waves, And Hydrodynamic Hierarchy

Sono-luminescence [D1], [D1] is a peculiar phenomenon, which might provide an application for the hydrodynamical hierarchy. The radiation pressure of a resonant sound field in a liquid can trap a small gas bubble at a velocity node. At a sufficiently high sound intensity the pulsations of the bubble are large enough to prevent its contents from dissolving in the surrounding liquid. For an air bubble in water, a still further increase in intensity causes the phenomenon of sono-luminescence above certain threshold for the sound intensity. What happens is that the minimum and maximum radii of the bubble decrease at the threshold and picosecond flash of broad band light extending well into ultraviolet is emitted. Rather remarkably, the emitted frequencies are emitted simultaneously during very short time shorter than 50 picoseconds, which suggests that the mechanism involves formation of coherent states of photons. The transition is very sensitive to external parameters such as temperature and sound field amplitude.

A plausible explanation for the sono-luminescence is in terms of the heating caused by shock waves launched from the boundary of the adiabatically contracting bubble [D1], [D1] . The temperature jump across a strong shock is proportional to the square of Mach number and increases with decreasing bubble radius. After the reflection from the minimum radius $R_s(min)$ the outgoing shock moves into the gas previously heated by the incoming shock and the increase of the temperature after focusing is approximately given by $T/T_0 = M^4$, where M is Mach number at focusing and $T_0 \sim 300$ K is the temperature of the ambient liquid. The observed spectrum of sono-luminescence is explained as a brehmstrahlung radiation emitted by plasma at minimum temperature $T \sim 10^5$ K. There is a fascinating possibility that sono-luminescence relates directly to the classical Z^0 force: this point is discussed in [K12].

Even standard model reproduces nicely the time development of the bubble and sono-luminescence spectrum and explains sensitivity to the external parameters [D1], [D1]. The problem is to understand how the length scales are generated and explain the jump-wise transition to sono-luminescence and the decrease of the bubble radius at sono-luminescence: ordinary hydrodynamics predicts continuous increase of the bubble radius. The length scales are the ambient radius R_0 (radius of the bubble, when gas is in pressure of 1 atm) and the minimum radius $R_s(min)$ of the shock wave determining the temperature reached in shock wave heating. Zero radius is certainly not reached since shock front is susceptible to instabilities.

Since p-adic length scale hypothesis introduces a hierarchy of hydrodynamics with each hydrodynamics characterized by a p-adic cutoff length scale there are good hopes of achieving a better understanding of these length scales in TGD. The change in bubble size in turn could be understood as a change in the "primary" condensation level of the bubble.

1. The bubble of air is characterized by its primary condensation level k. The minimum size of the bubble at level k must be larger than the p-adic length scale $L(k)$. This suggests that the transition to photo-luminescence corresponds to the change in the primary condensation level of the air bubble. In the absence of photo-luminescence the level can be assumed to be $k = 163$ with $L(163) \sim .76\ \mu m$ in accordance with the fact that the minimum bubble radius is above $L(163)$. After the transition the primary condensation level of the air bubble is $k = 157$ with $L(157) \sim .07\ \mu m$. In the transition the minimum radius of the bubble decreases below $L(163)$ but should not decrease below $L(157)$: this hypothesis is consistent with the experimental data [D1] , [D1].

2. The particles of hydrodynamics at level k have minimum size $L(k_{prev})$. For $k = 163$ one has $k_{prev} = 157$ and for $k = 157$ $k_{prev} = 151$ with $L(151) \sim 11.8\ nm$. It is natural to assume that the minimum size of the particle at level k gives also the minimum radius for the spherical shock wave since hydrodynamic approximation fails below this length scale. This means that the minimum radius of the shock wave decreases from $R_s(min, 163) = L(157)$ to $R_s(min, 157) = L(151)$ in the transition to sono-luminescence. The resulting minimum radius is 11 nm and much smaller than the radius .1 $\mu\ m$ needed to explain the observed radiation if it is emitted by plasma.

A quantitative estimate goes along lines described in [D1], [D1].

1. The radius of the spherical shock is given by

$$R_s = At^{\alpha} \ , \tag{3.15}$$

   where t is the time to the moment of focusing and α depends on the equation of state (for water one has $\alpha \sim .7$).

2. The collapse rate of the adiabatically compressing bubble obeys

$$\frac{dR}{dt} = c_0\left(\frac{2}{3\gamma}\frac{\rho_0}{\rho}\left(\frac{R_m}{R_0}\right)^3\right)^{1/2} \ , \tag{3.16}$$

   where c_0 is the sound velocity in gas, γ is the heat capacity ratio and ρ_0/ρ is the ratio of densities of the ambient gas and the liquid.

3. Assuming that the shock is moving with velocity c_0 of sound in gas, when the radius of the bubble is equal to the ambient radius R_0 one obtains from previous equations for the Mach number M and for the radius of the shock wave

$$\begin{aligned} M &= \frac{\frac{dR_s}{dt}}{c_0} = (t_0/t)^{\alpha-1} \ , \\ R_s &= R_0(t/t_0)^{\alpha} \ , \\ t_0 &= \frac{\alpha R_0}{c_0} \ . \end{aligned} \tag{3.17}$$

where t_0 is the time that elapses between the moment, when the bubble radius is R_0 and the instant, when the shock would focus to zero radius in the ideal case. For $R_0 = L(167)$ (order of magnitude is this) and for $R_s(min) = L(151)$ one obtains $R_0/R_s(min) = 256$ and $M \simeq 10.8$ at the minimum shock radius.

4. The increase of the temperature immediately after the focusing is approximately given by

$$\frac{T}{T_0} \simeq M^4 = (\frac{R_0}{R_s})^{\frac{4(1-\alpha)}{\alpha}} \simeq 1.3 \cdot 10^4 \ . \tag{3.18}$$

For $T_0 = 300\ K$ this gives $T \simeq 4 \cdot 10^6\ K$: the temperature is far below the temperature needed for fusion.

In principle the further increase of the temperature can lead to further transitions. The next transition would correspond to the transition $k = 157 \rightarrow k = 151$ with the minimum size of particle changing as $L(k_{prev}) \rightarrow L(149)$. The next transition corresponds to the transition to $k = 149$ and $L(k_{prev}) \rightarrow L(141)$. The values of the temperatures reached depend on the ratio of the ambient size R_0 of the bubble and the minimum radius of the shock wave. The fact that R_0 is expected to be of the order of $L(k_{next})$ suggests that the temperatures achieved are not sufficiently high for nuclear fusion to take place.

3.6 P-Adic Length Scale Hypothesis, Hydrodynamic Turbulence, And Distribution Of Primes

The work of Indian meteorologists Mary Selvam [H1] related to the turbulent atmospheric flows provides additional very interesting insight to p-adic length scale hypothesis and suggests that n-ary p-adic length scales corresponding to very large values of n are realized in hydrodynamical turbulence, and that hydrodynamical vortices could be regarded as elementary particle like objects on the space-time sheets at which they are condensed topologically.

1. The distribution of vortex sizes is same as distribution of primes

Selvam studies the distribution for the ratio $z = R/r$ of large vortex radius R to smallest vortex radius r, and finds that this distribution is the same as the distribution of primes in region of rather small primes. This could be understood if vortex radii are prime multiples of r

$$R = kr \ , \ k \ \text{prime} \ ,$$

and if each prime appears with the same probability. This assumption can be actually loosened: one can also interpret r as the p-adic length scale associated with minimum size vortex interpreted as space-time sheet. Selvam also argues that vortex dynamics has quantal features and that vortices could in some aspects be regarded as quantum objects.

2. p-Adic length scale hypothesis from elementary particle blackhole analogy

One can try to understand results on basis of the p-adic length scale hypothesis $p \simeq 2^{k^m}$, k prime, m positive integer.

1. At quantum level p-Adic length scale hypothesis follows from the generalization of Hawking-Bekenstein law for the radius of elementary particle horizon defined as the surface at which the Euclidian signature of the induced metric of the space-time sheet containing topologically condensed particle changes to Minkowskian signature of the metric in regions faraway from particle. Ordinary elementary particles corresponds to CP_2 type extremals condensed on larger space-time sheet with size of order $L_p = \sqrt{p}l$, $l \simeq 10^4$ Planck lengths. Generalized Hawking-Bekenstein law implies that the p-adic entropy of elementary particle characterized by p-adic prime p is proportional to the surface area of the elementary particle horizon. Since entropy is proportional to $log(p)$, the radius r of the elementary particle horizon satisfies $r^2 \propto log(p)$.

2. The idea is to require that the radius of the elementary particle horizon itself is m-ary p-adic length scale. For $p \simeq 2^{k^m}$ this is indeed the case if generalized Hawking-Bekenstein law holds and one has

$$r = \sqrt{k^m} \times l \ , \ k \ \text{prime} \ .$$

For $m = 2$ one has

$$r = kl \ .$$

This is the same law as holds true for the vortex radii except that l corresponds to Planck length scale rather than macroscopic size of the minimal vortex. Therefore a generalization replacing l with the size of the minimal vortex is needed.

3. Does generalization of Hawking-Bekenstein hold true also for vortices regarded as elementary particles?

One must be able to generalize the notion of elementary particle by allowing also larger space-time surfaces than CP_2 type extremals as models of particle and to assume that the metric of the space-time sheet at which particle is condensed has Euclidian metric signature inside the particle region, now inside the region covered by vortex.

1. A more general situation allowed by the p-adic length scale hypothesis corresponds to vortices topologically condensed at space-time sheets with size of order of n-ary p-adic length scale

$$L_p(n) = p^{n/2} L_p \ , \quad p \simeq 2^{k^m} \ .$$

In this case generalized Hawking-Bekenstein law implies that the radius of the elementary particle horizon is given by

$$r = k^m \times L \ , \quad L = \tfrac{n}{2} \times l \ .$$

$m = 2$ applies in the situation studied by Mary Selvam. Also the values of k can be small in this case. What is important is that the fundamental p-adic length scale l has been effectively replaced by $L = nl/2$. This is in accordance with the idea of fractality.

2. The requirement that r is also now p-adic length scale would imply that the length scale $k^m \times \frac{n}{2} \times l$ is p-adic length scale. This does not make sense except possibly as an approximation. p-Adic length scale hypothesis however suggests that the new fundamental length scale L itself is some n-ary p-adic length scale. The simplest possibility is that $n/2$ is large prime p_1 so that one has

$$n = 2p_1 \ , \quad r = p_1 l \ .$$

$L = p_1 l$ and clearly corresponds to the secondary p-adic length scale associated with p_1 satisfying itself p-adic length scale hypothesis $p_1 \simeq 2^{k_1^{m_1}}$. This assumption provides the scenario with strong predictive power since the number of the secondary p-adic length scales is not very high.

3. Does atmospheric turbulence provide a fractally scaled version of elementary particle physics?

In the length scale range between .1 meters and Earth circumference the following p-adic primes $p_1 = n/2$ are possible:

$$p_1 \simeq 2^{k_1^{m^1}} \ ,$$
$$k_1^{m^1} = 101, 103, 107, 109, 113, 11^2 = 121, 5^3 = 125, 127 \ .$$

There would be only 8 minimal vortex sizes in this length scale range, which is very strong and testable prediction. What is fascinating is that these secondary length scales correspond to the p-adic primes associated with quarks, atomic nuclei, and leptons so that the physics of vortices in atmosphere might in some sense be regarded as a fractal copy of elementary particle and nuclear physics! Note that the length scale $L(n,k)$ giving the size of the space-time sheet at which vortex is condensed, is given by

$$L(n,k^2) \simeq 2^{2^{k_1-1}\times k^2} \quad ,$$

and is completely super-astronomical already for small values of k.

4. Does the space-time region at which vortex is condensed have Euclidian metric signature?

What this model implies is that the induced metric at the space-time sheet at which vortex is condensed, should have Euclidian signature inside radius r. TGD indeed allows huge number of vacuum extremals with Euclidian signature: signature becomes Euclidian if the dependence of the CP_2 coordinates on M^4_+ coordinates is too fast. The simplest situation is encountered when the angle coordinate ϕ associated with CP_2 geodesic circle satisfies the condition $\phi = \omega t$, $\omega \geq 1/R$, where $2\pi R$ is the length of the CP_2 geodesic circle and t is Minkowski time coordinate. From this it is clear that time gradients must be typically larger than $1/R$, where R is CP_2 size, for Euclidization to happen. Also criticality of the preferred extremals of Kähler action (there exists infinite number of deformations with a vanishing second variation identifiable in terms of conformal symmetries) is consistent with the formation of Euclidian regions. Thus field equations support the idea that space-time sheets can contain Euclidian regions of even macroscopic size. Inside the region covered by the vortex light would not propagate at all and Euclidian regions would be in some respects analogous to black holes. Vortex space-time sheets itself would obey good old Minkowskian physics.

5. Connection with dark matter hierarchy

The remarks above were written much before the realization that TGD "predicts" a dark matter hierarchy with the values of Planck constant $\hbar(n) = \lambda^n \hbar(1)$, $\lambda = n/v_0 \simeq n \times 2^{11}$, $n = 1, 2, ...$ λ is predicted to be integer and also sub-harmonics could be allowed. This means that also the scaled up variants of the p-adic length scale hierarchy appears. For the preferred value of $\lambda \simeq 2^{11}$ precise predictions of preferred time and length scales corresponding to small values of p-adic primes follow. In particular, the TGD based interpretation [K10, K7] of Nottale's proposal [E1] for the quantization of planetary orbits in terms of a gigantic value of gravitational Planck constant means that huge scalings are possible so that quantum effects are present in astrophysical and even cosmological length scales. The proposed picture might be consistent with this view since also $\hbar(1)$ is predicted to have a discrete spectrum varying by a factor 2.

3.7 Thermodynamical Hierarchy

p-Adic TGD suggests the replacement of the ordinary thermodynamic description of the condensed matter with a hierarchy of p-adic thermodynamics, one for each p-adic level. Above the p-adic length scale $L(k)$ this thermodynamics is ordinary real thermodynamics. Below the length scale $L(k)$ p-adic thermodynamics is probably needed (assuming that thermodynamic description makes sense at all).

The general formulation might look like follows.

1. There is thermodynamics associated with each p-adic level of the condensate (in analogy with p-adic conformal field theory limit of TGD). The order parameters for ordinary condensed matter are particle densities at each level of the condensate. Besides this block densities describing the density of $p_1 < p_2$-adic blocks of matter at level $p_2 > p_1$ are present. Join along boundaries bonds/flux tubes give rise to bound state formation and corresponding densities can also be present. In spin systems also block densities for spin are present and can be identified as densities for magnetic domains with preferred sizes given by the p-adic cutoff length scales $L(k)$ given by prime powers of two.

2. The basic variational principle is the absolute minimization of free energy subject to certain constraints such as the constraint fixing total pressure: absolute minimization would be in

accordance with the absolute minimization of Kähler action (only one candidate for the characterization of preferred extremals) and implies the so called Maxwell rule for phase transitions. Free energy contains three parts: the "ordinary" free energy F_o, TGD based contribution to free energy and constraint term

$$F = F_{TGD} + F_o + F_{constraint} \ . \tag{3.19}$$

The "ordinary" free energy F_o at level p is sum of single particle free energies for p_1-adic blocks with $p_1 < p$ and the block-block interaction energies plus higher order interaction energies

$$F_o = \sum_i F_i + \sum_{ij} F_{ij} + ... \ . \tag{3.20}$$

The index $p_1 \simeq 2^k$, k prime, labelling different p_1-blocks is included in the index i. Ordinary thermodynamics suggests general forms for these terms. By fractality the various parameters appearing in free energies associated with different p-adic levels should be related by simple scaling laws. For instance, van der Waals type form should be appropriate for the free energy associated with a given block density of fluid at a given level of condensate. Also the general form for the block-block interaction terms can be guessed on general grounds.

The free energy has the general form

$$F_{TGD} = \sum_i N_i(-E_{cond} - E_{join}) + \sum_{ij} E^{ij}_{int} + F_{gr} \ . \tag{3.21}$$

The energy decomposes into a sum of the condensation energies $E_{cond} = \frac{b(k)}{L(k)}$ and join along boundaries/flux tube binding energies E_{join} for blocks and of Kähler interaction energy and gravitational binding energy. According to the previous arguments, gravitational binding energy becomes important only in length scales $L(k) > \frac{1}{T}$. Depending on whether the condensate level is of electromagnetic or Z^0 type Kähler interaction energy corresponds either to electromagnetic or Z^0 Coulomb energy. Also magnetic interaction energies are possible. The general order of magnitude estimate for Kähler interaction energy is obtained if one accepts the previously proposed general picture of the electromagnetically neutral topological condensate.

One can understand these terms as coming from the Boltzmann weight $exp(E_{cond} + E_{join} + E_{gr} - E_K)$ appearing in the partition function associated with p: th level of the condensate. Kähler interaction energy is actually thermal average of the Kähler interaction energy and contains small temperature dependence. Due to its smallness it seems however safe to neglect this dependence. There is also a second reason for separating the ordinary contributions and those present only in TGD framework. Ordinary free energy is related to short range interactions and is not sensitive to the finite size of the p-adic surface whereas Kähler interaction energy corresponds to long range interaction and depends strongly on the size of the p-adic surface.

Besides these terms also Lagrange multiplier terms, such as a term

$$F_{const} = \lambda(p_{ext} - \frac{\partial F}{\partial V}) \ . \tag{3.22}$$

fixing the pressure to the external pressure at the highest level of the condensate, are present. The condensation level at which the constraint term appears corresponds naturally to the length scale $L(k) \sim \frac{1}{T}$ determined by the temperature: above this length scales gravitational interaction dominates. At the lower levels of the condensate this kind of pressure term is not present and the minimization of free energy fixes completely the various densities at these levels of the condensate. The important consequence is that the density of say, fluid, at short length scales should be fixed completely by the minimization conditions and should not depend on the external pressure at all.

The external pressure changes the density of blocks but the not the density inside blocks. An exception is provided by solid phases, for which join along boundaries implies the formation of lattice so that only single block density is present for an ideal solid.

At high temperatures and in long length scales Kähler interaction energy and condensation energy are completely negligible in general. At low temperatures and short length scales as well as in critical systems the situation is different. The formation of supra phases and also of ordinary solids by join along boundaries operation provide examples of the situation, where the Kähler energy probably must be taken into account.

4 WCW Geometry And Phase Transitions

The definition of the WCW Kähler geometry has beautiful catastrophe theoretic interpretation. As a matter fact, catastrophe theory enters at two levels. First, Kähler function $K(X^3)$ is defined as the preferred extremal of Kähler action and associates a unique space-time surface $X^4(X^3)$ to a given 3-surface X^3. It can quite well happen that the preferred extremal of the Kähler action as a function of the varied parameters changes in discontinuous manner. Secondly, "quantum average effective space-times" correspond to the preferred extremals $X^4(X^3_{max})$ associated with the maxima of Kähler function as function of 3-surface and has so called zero modes as external control parameters and also now catastrophes are possible.

4.1 Basic Ideas Of The Catastrophe Theory

To understand the connection consider first the definition of the ordinary catastrophe theory [A2]. In catastrophe theory one considers the extrema of a potential function depending on dynamical variables x as function of external parameters c. The basic space decomposes locally into cartesian product $E = C \times X$ of control variables c, appearing as parameters in the potential function $V(c, x)$ and of state variables x appearing as dynamical variables. Equilibrium states of the system correspond to the extrema of the potential $V(x, c)$ with respect to the variables x and in the absence of symmetries they form a sub-manifold of M with dimension equal to that of the parameter space C. In some regions of C there are several extrema of potential function and the extremum value of x as a function of c is multi-valued. These regions of $C \times X$ are referred to as catastrophes. The simplest example is cusp catastrophe (see **Fig. 1**) with two control parameters and one state variable.

In catastrophe regions the actual equilibrium state must be selected by some additional physical requirement. If system obeys flow dynamics defined by first order differential equations the catastrophic jumps take place along the folds of the cusp catastrophe (delay rule). On the other hand, the Maxwell rule obeyed by the thermodynamic phase transitions, states that the equilibrium state corresponds to the absolute minimum of the potential function and the state of the system changes in discontinuous manner along the Maxwell line in the middle between the folds of the cusp (see **Fig. 1**). As far as discontinuous behavior is considered fold catastrophe is the basic catastrophe: all catastrophes contain folds as there "satellites" and one aim of the catastrophe theory is to derive all possible ways for the stable organization of folds into higher catastrophes. The fundamental result of the catastrophe theory is that for dimensions d of C smaller than 5 there are only 7 basic catastrophes and polynomial potential functions provide a canonical representation for the catastrophes: fold catastrophe corresponds to a third order polynomial (in the fold the two real roots become a pair of complex conjugate roots), cusp to fourth order polynomial, etc.. The development of the fold catastrophe means that the minimum of a potential function decomposes to two minima so that previous minimum becomes local maximum.

4.2 WCW Geometry And Catastrophe Theory

Consider now how catastrophe theory emerges from the definition of the Kähler function. The most obvious identification for the parameter space C would be as the space of all 3-surfaces in $H = M^4_+ \times CP_2$. In order to get rid of the difficulties related to $Diff^4$ invariance one must however restrict the consideration to 3-surfaces belonging to H_a: the set of 3-surfaces of $M^4_+ \times CP_2$ with constant M^4_+ proper time coordinate. The counterpart of the total space $E = C \times X$ can

be identified as the space of the solutions of the Euler Lagrange equations associated with Kähler action (one could consider all 4-surfaces but this is not necessary) and decomposes only locally into Cartesian product. Intuitively the space X corresponds to the time derivatives for the variables specifying the space X and in Hamiltonian formalism to the canonical momenta. If the initial value problem is well defined, the values of C and X coordinates specify the extremum uniquely. In TGD this is not in general true as the extremely large vacuum degeneracy of the Kähler action strongly suggests.

Potential function corresponds to the Kähler action restricted to the solution space of the Euler Lagrange equations. Catastrophe surface corresponds to the four-surfaces found by extremizing Kähler action with respect to the variables of X (time derivatives of coordinates of C specifying X^3 in H_a) keeping the variables of C specifying 3-surface X^3 fixed. Extremization with respect to time derivatives implies a phenomenon analogous to the Bohr quantization since canonical momenta cannot be chosen freely as in the ordinary initial value problems of the classical physics. When catastrophe occurs there are several extremizing 4-surfaces going through the given 3-surface: otherwise one obtains just the sought for preferred extremal.

The requirement that Kähler function (Kähler action in Euclidian space-time regions) corresponds to absolute minimum is just Maxwell's rule in infinite dimensional context and implies that phase transition type catastrophic quantum jumps are typical for TGD Universe. Cusp catastrophe provides a simple concretization of the situation (see **Fig. 1**) The set M ("Maxwell set")of the critical 3-surfaces corresponds to the Maxwell line of the cusp catastrophe and forms codimension one set in configuration space. For 3-surfaces near to the Maxwell set M small one parameter deformation in the direction normal to it can induce large deformation of the 4-surface associated with it. This implies initial value sensitivity with respect to the coordinate X_n associated with the normal direction. Kähler function itself is continuous on Maxwell surface and mathematical consistency requires that also Kähler metric is continuous on Maxwell surface. A good example of a catastrophic jump is provided by a topology changing quantum jump (3-surface decays to two disjoint 3-surfaces) identifiable as 3-particle vertex.

The present situation differs from the ordinary catastrophe theory in several respects.

1. The parameter space C is infinite dimensional so that there seems to be no hope of having finite classification for catastrophes in TGD Universe. Of course, all lower dimensional catastrophes are expected to be present in TGD, too.

2. Kähler action possesses vacuum degeneracy and one cannot exclude the possibility that the absolute minima of the Kähler action are degenerate: this implies further modifications to the standard picture of catastrophe theory.

3. Maxwell rule follows as a theorem in Quantum TGD whereas in ordinary catastrophe theory delay rule (jumps takes place along the folds) follows as a theorem. The latter implies that the description of phase transitions is not possible using the catastrophe theory associated with flows. These observations suggests that classical dynamics (for instance the classical dynamics associated with Kähler action) obeys delay rule whereas quantum dynamics obeys Maxwell rule and that the phenomena of super cooling and super heating are related to classical dynamics and ordinary phase transitions are induced by quantum fluctuations.

The existence of the catastrophes is implied by the vacuum degeneracy of the Kähler action. For example, for pieces of Minkowski space in $M^4_+ \times CP_2$ the second variation of the Kähler action vanishes identically and only the fourth variation is non-vanishing: these 4-surfaces correspond to the tip of the cusp catastrophe (see **Fig. 1**). There are also space-time surfaces for which second variation is non-vanishing for special deformations only and a hierarchy of subsets in the space of extremal 4-surfaces with decreasing degeneracy of the second variation defines the boundaries of the projection of the catastrophe surface to the space of 3-surfaces. By p-adic fractality there are good reasons to expect that there are catastrophes in all length scales so that the increase in p-adic resolution leads to emergence of new smaller catastrophes on a given portion of the catastrophe surface.

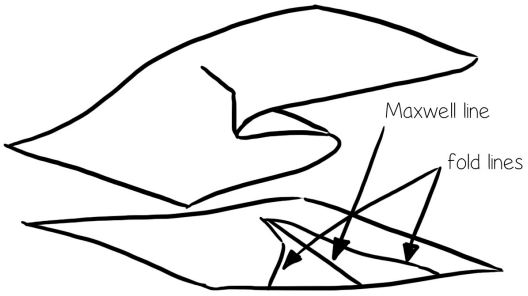

Figure 1: Cusp catastrophe

4.3 Quantum TGD And Catastrophe Theory

Catastrophes appear also in a second manner in TGD. As explained in the second part of the book, WCW allows an infinite number of zero modes. Zero modes characterize the size and shape of the 3-surface but do not appear in the line element of the configuration space metric. In good approximation WCW functional integrals associated with the S-matrix elements can in principle be calculated using perturbation theory around the maxima of the Kähler function and one can define "quantum average effective space-times" as the space-time surfaces $X^4(X^3_{max})$ associated with the maxima. Since the vacuum functional of the theory is the exponent of the Kähler function, the ill-defined Gaussian and metric determinants cancel each other and what remains is an integral over the zero modes. In general, for given values of the zero modes there are several maxima of the Kähler function and zero modes are in the role of the control parameters whereas the coordinates fixing the maximum of Kähler function for given values of the zero modes are in the role of the state variables. Also now infinite-dimensional catastrophe theory is in question.

The values of the vacuum functional at the Maxwell line of the cusp catastrophe same at the two sheets of the catastrophe but when one moves away from the Maxwell line, the second sheet begins to dominate due to the exponential dependence of the vacuum functional on Kähler function. One can also consider quantum jumps associated with the catastrophes: if the states represented by the points of the catastrophe surface are quantum entangled with the states of the external world or measurement apparatus E, one has, in the case of a cusp catastrophe, entanglement of the two sheets of the catastrophe with the states of E.

According to the strong form of Negentropy Maximization Principle, the quantum jumps selecting and of the sheets can occur when the quantum entanglement/entanglement entropy is large, actually largest in the set of all possible quantum subsystems. This is indeed the case at the Maxwell line, where the values of the Kähler function defining the entanglement probabilities at two sheets are identical so that entanglement entropy is maximized. Hence the region near the Maxwell line is predicted to be the region, where macroscopic phase transition like quantum jumps can occur and it is an intriguing possibility that thermal phase transitions basically correspond to this kind of quantum jumps. Strong form of NMP actually suggests that large number of nearly degenerate maxima must be involved so that the entanglement entropy becomes large.

4.4 TGD Based Description Of Phase Transitions

The above described mathematical structure should somehow reflect its presence also in the quantum description of the ordinary condensed matter phase transitions. Quantum criticality means that quantum states in TGD Universe are analogous to the states of a critical system and long range quantum correlations are predicted in all length scales. In principle, all quantum states are predicted to be critical in some time and length scale. The appearance of the join along boundaries-/flux tube condensates provides a concrete realization for quantum criticality. Spin glass analogy is in turn related to the enormous vacuum degeneracy of the Kähler action. This means the appear-

ance of infinite number of zero modes of the Kähler function, which characterize the size and shape of the 3-surface as well as the classical induced Kähler field and play the role of universal control parameters in the catastrophe theory. Zero modes are the quantum counterparts of macroscopic state variables, to which thermodynamical variables should reduce at quantum level, and clearly they have no counterpart in the ordinary quantum field theories.

The strong form of Negentropy Maximization Principle states that the quantum jump in a given quantum state is performed by a subsystem for which the quantum jump to an eigenstate of the density matrix gives maximum negentropy gain. There are good arguments suggesting that the second law of thermodynamics follows from the strong form of Negentropy Maximization Principle [K9].

1. State function reductions increase the negentropy of the subsystem in ensemble but only the subsystem for which negentropy gain is maximal, can make the quantum jump and reduce its entanglement entropy. In order to get the possibility to make quantum jump (and be conscious according to TGD inspired theory of consciousness), the subsystem must be able to generate entanglement entropy very effectively: therefore strong NMP favors the generation of entanglement entropy and, rather paradoxically, implies both evolution and the second law of thermodynamics as different sides of the same coin.

2. The maximum for the real counterpart of the p-adic entropy is proportional to $ln(p)$ and this implies that cosmological evolution leading to the emergence of larger p-adic length scales in the topological condensate favors also the increase of the entanglement entropy.

   Hence, *if* one can indeed identify thermal entropy as an entanglement entropy, there are good hopes that second law of thermodynamics follows as a consequence.

This picture leads to a straightforward generalization of Haken's non-equilibrium thermodynamics description of the self-organizing systems [B1] with configuration zero modes appearing in the role of the order parameters and the negative of the Kähler function playing the role of the potential function. The classical dynamics given by Langevin and Focker-Planck equations is replaced with the nondeterministic dynamics defined by quantum jumps. Quantum jump can be regarded as a basic step of self-organization.

As a special case, quantum description of the thermodynamical phase transitions should emerge. Quantum entanglement of the almost degenerate configurations near Maxwell line would be the purely quantal element of the quantum theory of phase transitions. The absolute minimization of the thermodynamical free energy and Maxwell rule would basically follow from the assumption that phase transition is induced by a quantum jump selecting between various maxima of the Kähler function and from the maximization of the Kähler function plus strong form of Negentropy Maximization Principle. The super cooling and super heating effects could be interpreted as produced by classical dynamics defined by the absolute minimization of the Kähler action for which the delay rule holds true. It must be however emphasized that absolute minimization of Kähler action is only one candidate identification of preferred extremals of Kähler action.

5 Embeddings Of The Cylindrically Symmetric Flows

In order to find orders of magnitude for the critical radii, the embeddings of some simple cylindrically symmetric flows will be considered. It is more convenient to consider Z^0 field instead of the Kähler field: these fields are proportional to each other for electrovac space-times: $J = pZ^0/6$ $(p = sin^2(\theta_W))$.

5.1 The General Form Of The Embedding Of The Cylindrically Symmetric Rotational Flow

In the following the flows at condensate levels $n \geq n_Z$ will be considered so that Z^0 fields are expected to dominate over the electromagnetic fields. Since the neutrinos screening the nuclear Z^0 charge are not expected to participate in the flow, only the Z^0 charge coming from level $n-1$ contributes to the spatial components of the Z^0 gauge current density at the level n and the time like component of the current density is therefore much smaller than the spatial components. This

motivates the study of the field configurations for which Z^0 electric field is negligibly small as compared to Z^0 magnetic field.

1. Theof em and Z^0 fields for vacuum extremals is given by $\gamma/Z^0 = -p/2$, $p = sin^2(\theta_W)$. Vanishing of the electromagnetic field is achieved for $p = 0$. It is indeed possible that Weinberg angle vanishes for vacuum extremals. The CP_2 projection of the embedding is two-dimensional, which implies the orthogonality of the magnetic and electric fields belonging to the same condensate level. On basis of the results of appendix Z^0 and em fields for vacuum extremals are given by

$$\begin{aligned} Z^0 &= (k+u)du \wedge d\Phi \ , \\ \gamma &= -\frac{p}{2}Z^0 \ . \end{aligned} \tag{5.1}$$

   Here $u = cos(\Theta)$ and Φ corresponds to spherical coordinates.

2. Z^0 charge density of matter is assumed to serve as a source of Z^0 fields and in the idealization that matter consists of identical nuclei (A, Z) one can write the charge density as

$$\rho_Z = -K_Z N_n \ , \ K_Z = \frac{g_Z^2}{4\sqrt{\epsilon_Z}}\frac{N}{A} \ . \tag{5.2}$$

   Here N_n is the density of nucleons and $N/\sqrt{\epsilon_Z}$ is the weak isospin per nucleus using neutrino isospin as a unit. ϵ_Z depends on the p-adic length scale involved and p-adic fractality suggests the scaling

$$\frac{N}{\sqrt{\epsilon_Z}} \propto N_0 \times (\frac{L(k_0)}{L(k)})^3 = N_0 \times 2^{-3(k-k_0)/2}$$

   as a function of $p \simeq 2^k$. Prime values of k are favored and $k = 113, 151, 157, 163, 167$ corresponding to Mersenne primes are especially interesting.

The general situation corresponds to a flow for which the matter rotates around the z-axis with velocity $\beta(\rho)$ and creates Z^0 magnetic field in the z-direction. The Z^0 magnetic field associated with the flow at n: th condensate level is given by

$$B^Z = K_Z N_n \int \beta(\rho) d\rho \ . \tag{5.3}$$

The spatial dependence of the Z^0 electric field is same as that of B^Z and this means that Z^0 charge density serving as the source of E^Z cannot be constant: a possible resolution of the problem is that the screening neutrinos at level n arrange themselves so that Z^0 charge density is not constant although the nucleon density is.

Using coordinates $(r, u = cos(\Theta), \Psi, \Phi)$ for CP_2, the cylindrically symmetric electromagnetically neutral embedding of this flow is obtained in the form

$$\begin{aligned} u &= u(\rho) \ , \\ \Psi &= \omega_2 m^0 + n_2\phi \ , \quad \Phi = \omega_1 m^0 + n_1\phi \ , \end{aligned} \tag{5.4}$$

where the relationship between the variables r and Θ is fixed by the vacuum extremal property (see Appendix of the book). The value of the parameter k is given by $k = \omega_2/\omega_1 = n_2/n_1$.

From the general expression for the Z^0 field in the vacuum extremal space-time one obtains the following differential equation for u:

$$\begin{aligned} B^Z &= (k+u)n_1\frac{\partial_\rho u}{\rho} \ , \\ &= K_Z N_n \int \beta(\rho)d\rho \ , \end{aligned} \tag{5.5}$$

which gives the relationship between u and ρ in the following form

$$\int (k+u)du = \frac{K_Z N_n}{n_1}\int d\rho\rho \int d\rho\beta(\rho) \ . \tag{5.6}$$

Assuming that $u=-1$ corresponds to the z-axis and the boundary of topological field quantum to $u=1$, one obtains an expression for the critical radius:

$$\begin{aligned} \int_0^{\rho_{cr}} d\rho\rho \int \beta(\rho)d\rho &= -\frac{n_1}{K_Z N_n}\times 2k \ , \\ K_Z &= \frac{g_Z^2}{4\sqrt{\epsilon_Z}}\frac{N}{A} \end{aligned} \tag{5.7}$$

An attractive possibility is that the structures associated with the ordinary hydrodynamic flow might be understood as consequences of CP_2 geometry. It will be found that the order of magnitude estimates give quantitative support for this guess.

One obtains also a quantization of Z^0 magnetic flux as

$$\int B_Z da = 2\pi n_1 \int (k+u)du = 4\pi k n_1 \ , \tag{5.8}$$

What is nice is that the quantization condition eliminates the dependence of the critical radius on the poorly known vacuum quantum numbers totally. The least one can hope is that the condition fixes orders of magnitude correctly.

p-Adic length scale hypothesis suggests a simple scaling for the flow velocities guaranteeing that ρ_{cr} scales as $L(k)$. $K_Z \propto L(k)^{-3}$ scaling, which follows from the assumption that the number of dark Z^0 charges per p-adic volume does not depend on p, implies the scaling

$$\int \beta_k(\rho)d\rho \propto L(k)^{-3}$$

achieved for

$$\beta_k(\rho) \propto (\frac{\rho}{L(k)})^k L(k) \ .$$

The decay of a structure characterized by the p-adic length scale $L(k)$ to smaller structures with smaller values of k could provide a general mechanism for generating fractal structures [A1]. The model of turbulence favors the scaling $2^k = 2^5$ for the vortices in the hierarchy. This scaling could also correspond to the Mersenne prime $M_5 = 2^5 - 1 = 31$.

CP_2 topology is bound to become important for large scale flows. The central ill understood problem in the astrophysics is the understanding of the turbulence and the dissipation of the angular momentum [E3]. From the foregoing it is clear that TGD approach might provide understanding concerning several astrophysical problems [E3]. An interesting test for the ideas is the possible existence of the nested fractal structures related by discrete scale transformations.

5.2 Orders Of Magnitude For Some Vacuum Parameters

The space-time associated with the flow is characterized by several parameters. Besides the parameters ω_i and n_i there are integer valued parameter m and the parameter u_0. In the following estimates for the general orders of magnitude for some of these parameters will be derived.

5.2.1 An estimate for the parameter ϵ_Z

The requirement that gravitational interaction is stronger than Z^0 force in long length scales implies $\epsilon_Z(n \to \infty) \geq 10^{36}$. At the condensate level $n = n_Z$ at which elementary particles feed their Z^0 charges the estimate

$$\epsilon_Z \sim 10^{20} \ ,$$

holds true by the argument related to the dissipation in super fluid flow, to be developed later. For the Z^0 magnetic field at level n the $\epsilon_Z(n-1)$, rather than $\epsilon_Z(n)$, appears in the expression of B_Z (assuming that dark neutrinos do not participate in the flow) so that at level $n = n_Z$ strong B_Z fields are possible ($\epsilon_Z = 1$).

5.2.2 An estimate for the quantum number n_1

An essentially similar estimate have been already carried out in the previous chapter. The requirement that angular momentum density is of correct order of magnitude, gives an estimate for the value of the parameter n_1. The expression of the conserved gravitational angular momentum current in the z-direction is given by

$$J^\alpha \ = \ T^{\alpha\beta}_{gr}\partial_\beta m^k m_{kl} j^l \ , \tag{5.9}$$

where j^k denotes the vector field associated with the infinitesimal rotation and $T^{\alpha\beta}_{gr}$ denotes gravitational energy momentum tensor defined by Einstein's equations. For the angular momentum density one obtains in the cylindrical M^4 coordinates for X^4 the expression

$$J^t \ = \ T^{t\phi}_{gr}\rho^2 \ . \tag{5.10}$$

The leading order contribution to the angular momentum density comes from the non-vanishing of the metric component

$$\begin{aligned} g_{t\phi} \ &= \ s^{eff}_{\Phi\Phi}\omega_1 n_1 = -\frac{R^2}{4}X \times \left[(1-X)(k+u)^2 + 1 - u^2\right]\omega_1 n_1 \ , \\ X \ &= \ D|k+u| \ , \ D = \frac{r_0^2}{1+r_0^2} \times \frac{1}{k+u_0} \ , \ r_0 = r(u_0) \ , \end{aligned} \tag{5.11}$$

and one obtains the order of magnitude estimate

$$J^t \ \simeq \ -T^{tt}_{gr} g_{t\phi}\rho^2 \simeq \rho_m \frac{R^2}{4}\omega_1 n_1 \ . \tag{5.12}$$

In order to obtain a correct order of magnitude for the angular momentum density associated with the rotational flow one must have

$$\frac{R^2}{4}\omega_1 n_1 \ \simeq \ \rho\beta(\rho) \ , \tag{5.13}$$

which implies

$$n_1 \ \simeq \ \frac{L}{R}\beta \ , \tag{5.14}$$

where L and β are the typical scale and velocity associated with the flow. It is clear that n_1 is an enormous number: essentially the size of the rotational flow measured using CP_2 length as a unit.

5.2.3 Estimate for ω_2, n_2 and m

The values of the parameters ω_2 and n_2 and m remain free and the attractive possibility is that the value of the parameter n_2 is small, perhaps of the order of one. If this the case then the value of the parameter ω_2 is also small

$$\frac{\omega_2}{\omega_1} = \frac{n_2}{n_1} \simeq \frac{R}{L}\frac{n_2}{\beta} \ . \tag{5.15}$$

The first guess is that at microscopic scales the order of magnitude for ω_2 corresponds to the p-adic lengths scale of dark matter particles in question and ω_1 is of order CP_2 mass as the embeddings of Schwartchild metric as a vacuum extremal suggest [K14]. $\omega_2 \sim m_e$ gives $n_2 \sim 10^{-19}(L/R)\beta$. For $L = 0.1$ meters and $\beta \simeq 10^{-8}$ one would have $n_2 \sim 10^6$.

5.3 Critical Radii For Some Special Flows

In order to get concrete picture of the situation it is useful to calculate the critical radius for some special flows.

5.3.1 Vortex flow

The velocity field is irrotational except on the z-axis and velocity and Z^0 magnetic fields are given by

$$\begin{aligned} \beta &= \frac{K}{\rho} \ , \\ B^Z &= K_Z N_n K ln(\frac{\rho}{\rho_0}) \ . \end{aligned} \tag{5.16}$$

Assuming that $r = 0$ on the z-axis, one obtains for the critical radius the equation

$$\rho_{cr}^2(ln(\frac{\rho_{cr}}{\rho_0}) - \frac{1}{2}) = -\frac{2n_1 k}{K_Z N_n K} \ . \tag{5.17}$$

To a logarithmic accuracy, this gives the order of magnitude estimate

$$\rho_{cr} = 2\sqrt{\frac{n_1 k}{K_Z N_n K}} \ . \tag{5.18}$$

The size of the critical radius decreases as the vorticity K increases.

5.3.2 Rigid body flow

Velocity field and Z^0 magnetic field are given by

$$\begin{aligned} \beta &= \Omega\rho \ , \\ B_Z &= K_Z N \Omega \frac{\rho^2}{2} \ . \end{aligned} \tag{5.19}$$

The value of the critical radius is given by the condition

$$\rho_{cr} = (\frac{16kn_1}{K_Z N_n \Omega})^{1/4} \ , \tag{5.20}$$

for the quantized Z^0 magnetic flux.

6 Transition To The Turbulence In Channel Flow

In sequel a general model for the transition to turbulent flow is proposed. In order to see whether the proposed scenario has anything to do with the reality it is useful to look whether one can understand the generation of a turbulence in some simple situation, which is chosen to be channel flow. The consideration is restricted to the length scales $L > \xi$ so that Z^0 magnetization should play key role in the generation of turbulence if the proposed general model is correct.

6.1 Transition To The Turbulence

In the following a general model for the transition to turbulent flow below length scale identifiable as a weak length scale characterizing dark weak bosons L_w associated with the largest vortices. Similar model might apply also in the case of magnetic fields. In the following the phrase "Kähler field" refers either to the ordinary electromagnetic field or Z^0 field or possibly to their linear combination depending on the context.

1. The probability of the configuration is proportional to the exponent of the Kähler function so that the most probable configurations correspond to a large value of the Kähler action. Kähler action can be increased by making either the magnitude of the Kähler electric part smaller or the magnitude of the Kähler magnetic part larger. The first mechanism is expected to be at work at non-relativistic velocities since the ratio of the Kähler magnetic and electric contributions to the Kähler action is expected to be of the order of β^2, where β is typical flow velocity. The transition to configuration with larger Kähler action is expected to take place provided it is energetically possible and is consistent with the minimization of the Kähler action.

2. Spontaneous Kähler magnetization provides the means to generate a positive action. The Kähler action of the Kähler magnetized space-time domain should be larger than that associated with the same domain without magnetization. It turns out that the Kähler electric action associated to a vortex region moving with the fluid has smaller magnitude than that associated with the same volume of the original flow: the reason is that Kähler electric field associated with the vortex is small near the core of the vortex. CP_2 geometry implies that the stable domains of the Kähler magnetization have some finite critical size. Kähler magnetized domains correspond to vortices and due to the viscosity, vortices grow until their achieve a critical size.

3. Vortex must get somehow rid of its angular momentum and kinetic energy and the topological quantum numbers n_1 and n_2 must become zero. One candidate for the region, where new vortices are produced is the region near the critical radius, where the velocity gradients are large so that the viscosity plays important role. The vortices created in this region cannot however lead to a decrease of n_1 and n_2. The process leading to a decrease of n_1 and n_2 is a generalization of the process known as phase slippage in super fluidity [D2]. Daughter vortices are created at the core of the mother vortex and they propagate under the action of Magnus and friction forces to the boundary of the mother vortex and carry away the quantum numbers n_1 and n_2 of the mother vortex gradually.

   For the flow $\beta = K/\rho$, which is irrotational outside the symmetry axis, which actually corresponds to a cylindrical hole of finite radius r, this hypothesis makes sense since the variation of velocity is large in normal direction in the core and dissipation rate therefore largest near the boundary of the hole. The radius r defines a natural lower bound for the sizes of vortices involved.

4. The transition to turbulence involves the generation vortices of various sizes related by scale transformations. That this is the case is suggested by the following argument. It is an empirical fact that the size of the daughter vortices is smaller than the size of mother vortex (this assumption forms the basis of Kolmogorov and Heisenberg theories of turbulence [B3]). The conservation laws of energy and angular momentum however imply that daughter vorticities cannot be larger than mother vorticity. The critical radii of the mother and daughter vortices are related by the scale transformation $\rho_{cr} \to \lambda\rho_{cr}$. λ is expected to be a

negative power of 2 and it turns out that $\lambda < 2^{-5}$ is consistent with the Heisenberg's model for the generation of turbulence. In fact, a distribution $\lambda(k) = 2^{-k}$, $k \geq 5$, for vortex sizes might be allowed.

The hypothesis that vortex decay corresponds to a decay of higher levels in the dark matter hierarchy by de-coherence such that $\hbar$ is reduced by could a factor $\lambda = v_0/n \simeq 2^{-11}/n$, $n = 1, 2, ...$, is consistent with the proposal. The decay would correspond to a decay of Bose-Einstein condensates of corresponding weak bosons to those at the lower level of darkness and thus having Compton lengths reduced by λ.

5. The transition to turbulence can be understood as a a fractal like process. In the case of the channel flow, the walls serve as sources of the mother vortices with large critical radii. These vortices in turn decay to smaller vortices. At a given condensate level the process stops, when the size of the daughter vortices is so small that the hydrodynamics approximation fails so that the radius of the smallest vortices is of same order of magnitude as the length scale $L(n)$ giving the size of smallest structures at the condensate level in question. A necessary condition for the process to occur is that the total Kähler action generated is positive. The criterion for the process to occur is that the total Kähler action associated with the cascade is positive.

It should be emphasized that the decomposition of the space-time into above described regions is very general phenomenon characteristic for TGD. It happens for a general space-time with vanishing electromagnetic fields and also for more general space-time surfaces: the condition in question might state the vanishing of the Kähler field or electromagnetic field or the proportionality of the Kähler field and electromagnetic field. This suggests rather unexpected support for the basic assumptions of TGD: many of the fractal structures encountered in Nature might be direct manifestations of CP_2 geometry!

6.2 Definition Of The Model

The transition to turbulence is cascade process.

1. Mother vortices having initial radius ρ_0 are created at the walls of the channel, where the velocity gradients are large and viscosity plays important role. Let ξ is the length scale above which hydrodynamic approximation works. ξ should be of the order of atomic length scale $a = 10^{-10}$ m.

   In the rest frame of the vortex the velocity field is given by

   $$\beta(\rho) = \frac{K}{\rho} . \tag{6.1}$$

   The sign of the vorticity is such that the formation of the vortices tends to make velocity zero at the walls of the channel.

2. Mother vortices move across the channel under the combined action of the Magnus force $F = K \times v$ and friction force and reach a critical size. Mother vortices dissipate their energy and angular momentum by the emission of daughter vortices by the phase slippage process. The critical radius of the daughter vortices is by a factor λ smaller than the critical radius of the mother vortex. The value of λ remains a parameter to be fitted.

3. The process repeats itself until the size of the daughter vortices is of the order of ξ and hydrodynamic approximation fails.

6.3 Estimates For The Parameters

Consider now a more quantitative definition of the process.

1. The order of magnitude estimates for the parameters $k(0) \equiv k$ and $\rho_{cr}(0) \equiv \rho_1$ are obtained in the following manner.
   i) ρ_1 should be smaller than the width of the channel for obvious geometric reasons:

$$\rho_1 \quad \leq \quad d \ . \tag{6.2}$$

   This same estimate follows from the requirement that the configuration with a vortex possesses larger Kähler action than the configuration without any vortex as will be found later.
   ii) An upper bound for the vorticity K is obtained by requiring that the flow velocity at $\rho \simeq \xi$ is not larger than the thermal velocity (sound velocity could be taken as an alternative lower bound: orders of magnitude are same): $K/\xi \leq \beta_{th}$, which gives

$$K \quad \leq \quad K_{max} \simeq \xi\beta_{th} \ . \tag{6.3}$$

2. A natural requirement is that the rotation velocity of the vortices at the critical radius is of the same order of magnitude as the velocity of the main flow

$$\frac{K}{\rho_1} \quad \simeq \quad \beta \ . \tag{6.4}$$

   This condition guarantees that the angular momentum of the vortex is of the same order of magnitude as the angular momentum for the main flow in the vortex region. Substituting this constraint and the upper bound for k to the condition $\rho_1 \leq d$ one obtains Reynolds number type criterion

$$\frac{\beta d}{\nu} \quad \geq \quad R_{cr} \equiv \frac{\beta_{th}\xi}{\nu} \ , \tag{6.5}$$

   when the vorticity K is maximal ($K \simeq \xi$ in units $c = 1$).

3. A kinetic theory estimate for the order of magnitude estimate of the gas viscosity gives a correct order of magnitude in case of the small viscosity liquids, too and is given by

$$\nu \quad \simeq \quad \frac{\beta_{th}}{N\sigma} \ , \tag{6.6}$$

   where N is the density of nucleons in the liquid. Typically one has $N \simeq 10^{30}/Am^3$ (A is atomic mass number) and $\sigma \sim a^2$, $a = 10^{-10}$ m is atomic cross section: $\sigma \simeq 10^{-20}\ m^2$ holds true for liquids at room temperature.

4. Using the order of magnitude estimate for the kinematic viscosity ν one obtains

$$R_{cr} \quad = \quad \frac{\beta_{th}\xi}{\nu} \simeq N\sigma\xi \simeq Na^3\xi \sim \frac{10^4}{A} \times \frac{\xi}{a} \ . \tag{6.7}$$

   For $\xi \sim a$ the value of R_{cr} is of the correct order of magnitude since the fully developed turbulence sets in at Reynolds numbers of this order of magnitude. In case of water more careful estimate using the actual value of the kinematic viscosity and thermal velocity in room temperature gives $R_{cr} \simeq 1200 - 12000$.

According to this criterion turbulence can develop also for smaller Reynolds numbers by vortices with $K \leq d \leq \xi\beta_{th}/\beta$ (as it does) but not all vorticities allowed by the velocity condition are possible. For the critical Reynolds number means that all possible vorticities allowed by $\beta(\xi) \leq \beta_{th}$ are allowed and for larger Reynolds numbers the upper limit for the size of vortices: $\rho_{cr} \leq \xi\beta_{th}/\beta \leq d$ is strictly smaller than the width of the channel.

The critical Reynolds number follows from the geometric condition $\rho_{cr} \leq d$ in the case of a channel flow. It will be later found that the same condition follows also from the requirement that the generation of the vortex increases the Kähler action so that same kind of condition is expected also in case of, say, the flow between two rotating disks.

6.4 Kähler Fields Associated With The Cascade Process

In the following a simple model for the Kähler electric and magnetic fields associated with the main flow and vortices will be constructed. The following simplifying assumptions about the flow are made:
i) The flow takes place in a channel of height h, width d and length L.
ii) The flow velocity β is constant throughout the channel.
iii) The main flow has a constant density $\rho_m \equiv Nm_p$, possesses kinematic viscosity ν and thermal velocity β_{th}.

Consider first the Kähler electric and magnetic fields associated with the main flow and a vortex assumed to have its axis in the z-direction.

1. When the fluid is at rest, it creates Kähler electric field, which near the symmetry axis of the flow is cylindrically symmetric for long and wide channel is in the z-direction and given by

$$\begin{aligned} E^K_\rho &= K_Z N_n \frac{\rho}{2} \ , \\ K_Z &= \epsilon_1 10^{-19} \ . \end{aligned} \tag{6.8}$$

   Near the walls $x = d$ and $x = 0$ and far from the corners, the Kähler electric field is to a good approximation orthogonal to the wall and given by the expression

$$E^K_x = K_Z N_n (x - \frac{d}{2}) \ . \tag{6.9}$$

   Same applies on the walls $z = 0$ and $z = h$. The small effects caused by the density gradients on the Kähler electric field, are neglected.

2. The Kähler magnetic field near the axis of the symmetry has circles as its flow lines and the magnitude of the field is given by

$$B^K_\phi = K_Z N_n \beta \frac{\rho^2}{2} \ . \tag{6.10}$$

   Near the walls $x = d$ and $x = 0$ and sufficiently far from the corners the Kähler magnetic field is given by the expression

$$B^K_z = K_Z N_n \beta (x - \frac{d}{2}) \ . \tag{6.11}$$

3. The Kähler magnetic field created by the locally irrotational vortex vortex is given by the expression

$$B^K_z = K_Z N_n K ln(\frac{\rho}{\rho_0}) \ . \tag{6.12}$$

4. The Kähler electric field created by the vortex can be estimated by assuming the simplest possible embedding with vanishing electromagnetic fields ($\Psi = \omega_2 m^0 + n_2\phi$ and $\Phi = \omega_1 m^0 + n_1\phi$). The relationship between Kähler electric field and Kähler magnetic field is given by

$$\begin{aligned} E_\rho^K &= \frac{\omega_1}{n_1} B_z^K \rho \\ &= \frac{\omega_1}{n_1} K_Z N_n K ln(\frac{\rho}{\rho_0}) \simeq K_Z N_n ln(\frac{\rho}{\rho_0})\rho \ , \end{aligned} \tag{6.13}$$

and apart from the logarithmic factor behaves like the field created by a constant charge density. The last estimate is obtained using the previous order of magnitude estimate for the size of the integer n_1: $n_1 \simeq K/\sqrt{G}$. From this relationship one obtains an estimate for S_B^2/S_E^2:
$S_B^2/S_E^2 \simeq K^2/\rho_{cr}^2 \ll 1$.

6.5 Order Of Magnitude Estimate For The Change Of The Kähler Action And Reynolds Criterion

In the following a rough order of magnitude estimate for the various contributions to Kähler action and numerical criteria for the transition to the turbulence are derived. The estimates are based on the following assumptions.

1. The Kähler fields associated with the moving vortices are obtained by Lorentz boosts leaving the Kähler action of the vortex invariant.

2. Kähler magnetic contributions to the Kähler action are neglected so that the increase of the Kähler action must result from the decrease of the magnitude of the Kähler electric part of the action. This is indeed expected to take place since the Kähler electric field of the vortex is small near the vortex core.

3. The Kähler action resulting from the interaction of the main flow and vortex is neglected. For the Kähler electric part of the action this assumption is well founded by the symmetry considerations. The Kähler electric field of the vortex is radially symmetric and in the region, where this field has a considerable magnitude, the Kähler field of the main flow is constant to a good approximation so that the integral $\int E_{vortex} \cdot E_{flow} d^4x$ vanishes to a good approximation. The corresponding magnetic interaction term can be neglected by its smallness.

As a consequence the change in the Kähler action is simply the change in the Kähler electric contribution to Kähler action, when the Kähler electric field of the main flow is replaced with the Kähler electric field of the vortex inside the space-time volume occupied by the vortex and the condition for the generation of turbulence reads as

$$\delta S_E^K = S_E^K(vortex) - S_E^K(flow) \geq 0 \ . \tag{6.14}$$

For the vortex of $n:th$ generation $S_E^K(n)$ has order of magnitude given by

$$\begin{aligned} S_E^K(n) &= \frac{1}{16\pi\alpha_K} \int E_n \cdot E_n d^4x \\ &\propto K_Z^2 N_n^2 (\rho_{cr}^4(n)) h \frac{\pi}{4} \tau(n) \ , \end{aligned} \tag{6.15}$$

where $\tau(n)$ is the average lifetime of the n: th generation vortex. The value of $S_E^K(flow)$ near the wall has order of magnitude given by the expression

$$\begin{aligned} S_E^K(flow) &= \frac{1}{16\pi\alpha_K} \int E_{flow} \cdot E_{flow} d^4x \\ &\propto K_Z^2 N_n^2 d^2 (\rho_{cr}^2(n)) h \frac{\pi}{4} \tau(n) \end{aligned} \tag{6.16}$$

to a logarithmic accuracy. From the condition $S^K(vortex) \geq S^K(flow)$ one obtains to the same logarithmic accuracy

$$\rho_{cr}(n) \quad \leq \quad d \ , \tag{6.17}$$

which is identical to the condition obtained by a purely geometric argument. The condition is satisfied for all vortices in the cascade if it is satisfied for the initiating vortex.

Some comments on the condition is in order.

1. The condition poses an upper bound for the vorticities of the mother vortices: $K \leq \beta d$ in addition to the bound $K\xi \leq \beta_{th}$ and implies for the vortices with the maximal vorticity the condition $\beta d/\nu \geq 2/\beta_s$ as found already earlier. This means that full turbulence becomes possible at critical Reynolds number. Partially developed turbulence is possible for smaller Reynolds numbers, too. The vortices with the largest vorticity increase Kähler action most effectively and this suggests that the ordinary dissipation for a non-turbulent flow corresponds to the formation of small mother vortices.

2. Also flows without turbulence are possible since the condition states only that the most probable flows are turbulent. This is indeed what has been observed in the case of real flows: by appropriate experimental arrangements one can hinder the development of the turbulence up to rather high Reynolds numbers.

3. The critical Reynolds number derived from the requirement of large Kähler function has a correct order of magnitude for laboratory scale flows: $R_{cr} \sim \frac{10^4}{A} \times \frac{\xi}{a}$ ($R_{cr} \sim 10^4/A$ at room temperature).

4. The result is insensitive to the details of the cascade model since the first vortex serves as the bottle neck of the cascade.

6.6 Phase Slippage As A Mechanism For The Decay Of Vortices

6.6.1 Phase slippage in TGD context

Vortices must somehow dissipate their energy and angular momentum. Since angular momentum is proportional to the integer n_1 this means that some mechanism for reducing the value of n_1 must exist. This kind of mechanism is indeed known in the context of super fluidity and known as phase slippage [D2]. In case of the channel flow phase slippage means that the order parameter χ, which is completely analogous to the angle variables Ψ and Φ, develops in the following manner.

The original linear behavior $\chi = kx$, where x is the coordinate in the direction of flow is gradually deformed to a behavior for which χ changes by a multiple of 2π at single point $x = x_0$ and behaves otherwise linearly (see **Fig. 2**). Since χ and $\chi + n2\pi$ correspond to the same physical situation the result means that one replace the graph of χ with graph without the jump. This process implies dissipation: the value of the momentum like quantum number k has decreased by a discrete amount. Physically the phase slippage corresponds to the propagation of a vortex across the channel although this is not quite obvious: the quantized vorticity of the vortex is n/M so that vorticity is conserved in the process (see **Fig. ??**).

In the present context the phase slippage process has a nice geometric interpretation. A pair of $r = \infty$ and $r = 0$ surfaces is generated in the process. Ψ (Φ) can change discontinuously on the these surfaces and Ψ (Φ) indeed changes by a multiple of 4π (2π) and a phase slippage is generated. In present case it is quite obvious that this process corresponds to a propagation of a vortex across the channel.

The process can be generalized to provide a dissipation mechanism for the vortices. Daughter vortex is generated on the core of the decaying vortex and moves under the action of Magnus and friction forces in radial direction and finally leaves mother vortex. The quantum numbers n_1 and n_2 associated with the process are conserved.

$$n_k(mother, i) \quad = \quad n_k(mother, f) + n_k(daughter) \ , \quad k = 1, 2 \ . \tag{6.18}$$

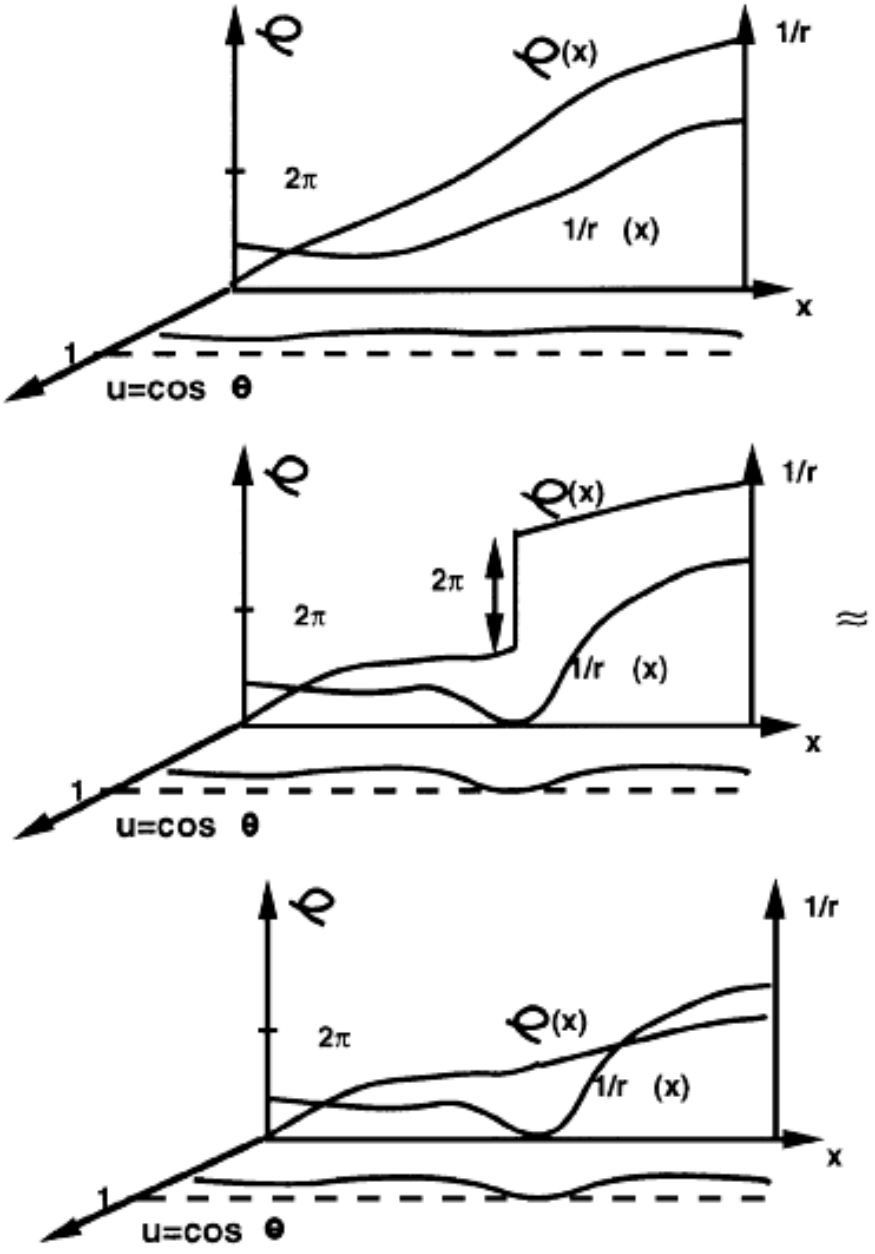

Figure 2: Phase slippage process and CP_2 geometry

If one assumes that K and n_1 are proportional to each other as they should be by the semiclassical argument, the critical radius of the mother vortex doesn't change in the process. If this process repeats itself sufficiently many times n_2 and n_1 become zero gradually resulting in a complete dissipation for the energy and angular momentum of the original vortex.

6.6.2 A model for the emission of the daughter vortices

A natural manner to model the emission of daughter vortices is as a stochastic process. Vortices are characterized by the quantum label $\Lambda = (n_1, n_2, \omega_1, \omega_2, m)$ and phase slippage corresponds to the emission process

$$\Lambda_1 \quad \rightarrow \quad \Lambda_2 + \Lambda_3 \ , \tag{6.19}$$

characterized by the decay rates

$$\Gamma(\Lambda_1 \rightarrow \Lambda_2 + \Lambda_3) \ . \tag{6.20}$$

Also the reverse process is possible but there are good reasons to assume that the fusion of the two vortices is a rather rare process.

It is straightforward to write general kinetic equations for the distribution of vortices as a function of Λ and in particular, as a function of the critical radius: this in turn leads to the distribution of the kinetic energy of the vortex as function of the the size of the vortex predicted also in the Heisenberg model for turbulence [B4, B3]. In order to get grasp of the situation it is however useful to make some simplifying assumptions about the decay of the vortices.

1. Vortex growth is a rapid process as compared to the motion of vortex between the core and the boundary of the mother vortex. This implies that the integer m associated with the daughter vortex must be smaller than the integer associated with the mother vortex. For simplicity it is assumed

$$m(daughter) \quad = \quad m(mother) - 1 \ . \tag{6.21}$$

2. The ratio $n_1/n_2 = \omega_1/\omega_2$ remains constant in the decay process if possible: this implies that the change in the functional relationship between CP_2 coordinates u and r is minimized. Since the ratio n_1/k is constant by a semiclassical argument implying that angular momentum is proportional to n_1, the conservation law

$$\frac{n_i}{k} \quad = \quad constant \ , \tag{6.22}$$

holding true for all vortices of the cascade is suggestive.

3. The conservation law implies that the critical radius, vorticity and and n_i of the daughter vortex are given by

$$\begin{aligned} \rho_{crit}(daughter) &= \lambda \rho_{crit}(mother) \ , \\ k(daughter) &= \lambda k(mother) \ , \\ n_i(daughter) &\simeq \lambda n_i(mother) \ , \\ \lambda &= 2^{-x} \ . \end{aligned} \tag{6.23}$$

The value of x is expected to be integer and will be fixed by the comparison with experiment.

The assumption

$$k(daughter) = \lambda k(mother) \ ,$$

makes sense if one gives up the assumption that magnetic flux is quantized irrespective of the value of n_1 as is clear by looking at the expression Eq. (5.18) for the critical radius for the vortex flow. One can however allow the increase of n (n_1 is multiple of n rather than arbitrary integer):

$$n(daughter) = \frac{n(mother)}{\lambda^2} \ ,$$

as is clear from the formula for the critical radius to achieve the quantization of magnetic flux. If magnetic flux quantization is assumed with the parameter $n = 1$ (n_1 integer) one must have

$$k(daughter) = \frac{k(mother)}{\lambda} \ ,$$

in order to get the critical radius correctly. The increase of k might be forced by the angular momentum conservation: if daughter vortices are created on the boundary of the mother vortex (as implied by the geometric picture) in the layer of a thickness $\rho_{crit}(daughter)$, the requirement that the angular momentum of the daughter vortices is of same order of magnitude as that of mother vortex, implies the desired formula. One must however remember that this argument need not make sense since flow equilibrium rather than decay of single vortex is in question. Also the increase of the average rotation velocity in small length scales looks un-physical feature. In any case, there are two possible scenarios:

$$\begin{array}{l} \text{a) Quantized magnetic flux and } n_i/k = constant: \ , \\ k(daughter) = \lambda k(mother) \ , \\ n(daughter) = \frac{n(mother)}{\lambda^2} \ , \\ \\ \text{Quantized magnetic flux and } n = 1: \\ k(daughter) = \frac{k(mother)}{\lambda} \ , \end{array} \tag{6.24}$$

and the scenario 1) looks more attractive.

For the mother vortex the corresponding quantities are after the decay given by

$$\begin{aligned} \rho_{crit}(mother, f) &= \rho_{crit}(mother, i) \ , \\ k(mother, f) &= k(mother, i)(1-\lambda) \ , \\ n_i(mother, f) &\simeq n_i(mother, i)(1-\lambda) \ . \end{aligned} \tag{6.25}$$

The process stops, when the condition $n_2(mother, f) = n_2(1-\lambda)^{N_f} \leq \lambda$ (n_2 refers to the mother vortex created at the wall) is satisfied, which gives the estimate

$$N_f(n_2) \simeq \frac{(ln(n_2) + ln(\lambda))}{|ln(1-\lambda))|} \ , \tag{6.26}$$

for the total number of the daughter generations with $m(daughter) = m(mother) - 1$ born in the dissipation of the mother vortex by the emission of the daughter vortices.

6.6.3 The distribution of the vortices as a function of the critical radius

Consider now the evaluation of the distribution for the number $N(\rho)$ of the vortices as function of the critical radius ρ.

1. The number of the daughters in the k: th generation having is given by

$$\begin{aligned} N_d(k) &\simeq \prod_{i=0}^{i=k} N_f(i) \ , \\ N_f(i) &= \frac{(ln(n_2) + (i+1)ln(\lambda))}{|ln(1-\lambda))|} \ . \end{aligned} \tag{6.27}$$

2. The size distribution is obtained by expressing the number k of generations in terms of the critical radius

$$k = -\frac{ln(\rho_m/\rho))}{ln(\lambda)} \ . \tag{6.28}$$

Here ρ_m denotes the initial value of the vortex radius created at the wall of the channel. Assuming that the size distribution $N(\rho_m)$ for the mother vortices emitted at the wall is known, one obtains the following expression for the size distribution of vortices

$$\begin{aligned} N(\rho) &= \int N(\rho|\rho_m) N(\rho_m) d\rho_m \ , \\ N(\rho|\rho_m) &= \prod_{i=0}^{k} N_f(i) \ , \\ N_f(i) &= \frac{(ln(n_2) + (i+1)ln(\lambda)}{|ln(1-\lambda)|} \ . \end{aligned} \tag{6.29}$$

An approximate expression of $N(\rho/\rho_m)$ holding true for small values of ρ is given by

$$\begin{aligned} N(\rho|\rho_m) &\simeq D(\frac{\rho_m}{\rho})^{\alpha+1/ln(\lambda)} \ , \\ D &= B^{-\frac{B}{ln(\lambda)}} A^{\frac{A}{ln(\lambda)}} \ , \\ A &= ln(n_2) + ln(\lambda) \ , \\ B &= A + ln(\frac{\rho}{\rho_m}) \ , \\ \alpha &= -\frac{ln(-\frac{1}{ln(1-\lambda)})}{ln(\lambda)}) \simeq 1 \ . \end{aligned} \tag{6.30}$$

D is a slowly varying logarithmic factor so that $N(\rho_m|\rho)$ behaves as the power $\rho^{1+\frac{1}{ln(\lambda)}}$ for all values of ρ_m. This implies that for small radii the general form of the size distribution is universal

$$N(\rho) \simeq C(\frac{\rho_m}{\rho})^{\alpha+\frac{1}{ln(\lambda)}} \ , \tag{6.31}$$

where C is some constant, which is determined once the rate of the energy dissipation is known.

The distribution of the kinetic energy of vortex per mass density ρ_m as a function of the vortex radius ρ can be evaluated using the formula

$$\frac{T(\rho)}{\rho_m} = \pi \int_0^{\rho} \beta^2(\rho) \rho d\rho \ . \tag{6.32}$$

1. For $\beta = K/\rho$ one obtains at the limit of the small radii

$$T(\rho) = C\pi K^2 ln(\frac{\rho}{\rho_0})(\frac{\rho}{\rho_0})^{\alpha+\frac{1}{ln(\lambda)}} \quad . \tag{6.33}$$

The leading order behavior of the Fourier transform of the energy function defined as $\hat{T}(p) \equiv \int exp(ip\rho)T(\rho)d\rho$ is for small values of the wave vector given by

$$\begin{aligned} \hat{T}(p) &\simeq p^{\Delta} \ , \\ \Delta &= -1-\alpha-\frac{1}{ln(\lambda)}) \ . \end{aligned} \tag{6.34}$$

2. For $\beta = \Omega\rho$ one obtains

$$\begin{aligned} T(\rho) &= C\pi\Omega^2(\frac{\rho}{\rho_0})^{4+\alpha+\frac{1}{ln(\lambda)}} \ , \\ \Delta &= -4-\alpha-\frac{1}{ln(\lambda)} \ . \end{aligned} \tag{6.35}$$

In the Heisenberg model for the turbulence [B4, B3] a similar form is obtained and the exponent is in that case equal to $\Delta = -5/3$ and experimentally verified in some cases. It should also be noticed that according to [B4] the assumptions implying $\Delta = -5/3$ in the Heisenberg model are not strictly true for the small values of the vortex radii. On basis of this result it seems that the values of $\Delta(TGD) = -4-\alpha+\frac{1}{ln(\lambda)}$ are un-physical in the case of the rigid body flow.

Only the flow $\beta = K/\rho$ predicting constant Z^0 magnetic field apart from logarithmic corrections predicts physically acceptable values of Δ. For $\lambda = 2^5$ one would have $\Delta(TGD) = -1-\alpha-\frac{1}{ln(\lambda)} \simeq -1.709$ to be compared with $-5/3 = -1.667$ of the Heisenberg model. The deviation from the prediction of Heisenber model is 2.5 per cent. The prediction does not depend strongly on the value of of the $\lambda = 2^{-x}$ and at the limit $x = \infty$ one has $\Delta = -2$. Hence a statistical distribution for the p-adic scalings involved with the decay does not affect dramatically the prediction.

The general vision about dark matter hierarchy characterized by the values of Planck constant given by $\hbar(n) = \lambda^{-n}\hbar(1)$, $\lambda = v_0/n \simeq 2^{-11}/n$, n integer, encourages to consider the possibility that the scaling is associated with a transition $\hbar(n) \to \hbar(n-1)$ to a lower level in the dark matter hierarchy accompanied by the reduction of Compton lengths and Compton times by factor λ. The decay to smaller vortices would correspond to a reduction of quantum coherence via a decay of dark weak bosons to lower level dark weak bosons. For $n = 1$ one has $\Delta = -1.869$. For $n = 3$ one would have $\Delta = -1.885$.

REFERENCES

Mathematics

[A1] Mandelbrot B. *The Fractal Geometry of Nature* . Freeman, New York, 1977.

[A2] Zeeman EC. *Catastrophe Theory.* Addison-Wessley Publishing Company, 1977.

Theoretical Physics

[B1] Haken H. *Information and Self-Organization.* Springer Verlag, Berlin, 1988.

[B2] Pitaevski LP Lifshitz EM. *Relativistic Quantum Theory: Part 2.* Pergamon Press, 1974.

[B3] Stanisic MM. *The Mathematical Theory of Turbulence.* Springer Verlag, 1985.

[B4] Shaffman PG. *Topics in Nonlinear Physics.* Springer Verlag, 1968.

Particle and Nuclear Physics

[C1] Barber BR et al. *Phys Rev*, 72(9):1380, 1994.

Condensed Matter Physics

[D1] Barber BR et al. *Phys Rev*, 72(9):1380, 1994.

[D2] Anderson PW. *Rev Mod Phys*, 38, 1966.

[D3] Tilley K Tilley DR. *Super Fluidity and Super Conductivity.* Adam Hilger Ltd, 1986.

Cosmology and Astro-Physics

[E1] Nottale L Da Rocha D. Gravitational Structure Formation in Scale Relativity, 2003. Available at: `https://arxiv.org/abs/astro-ph/0310036`.

[E2] Zirin H. *Astrophysics of the Sun.* Cambridge University Press, Cambridge, 1988.

[E3] Katz JI. *High Energy Astrophysics.* Addison Wesley Publishing Company, 1987.

Fringe Physics

[H1] Selvam AM. Quantum-like Chaos in Prime Number Distribution and in Turbulent Fluid Flows, 2000. Available at: `https://arxiv.org/abs/physics/0005067`.

[H2] Nieminen R Podkletnov E. Weak gravitational shielding properties of composite bulk YBa2Cu3O7-x super-conductor below 70 K under electro-magnetic field, 1992. Available at: `https://arxiv.org/abs/cond-mat/9701074`. Report MSU-chem 95, improved version at `https://arxiv.org/abs/cond-mat/9701074`.

Biology

[I1] Murogoki P Comorosan S, Hristea M. On a new symmetry in biological systems. *Bull Math Biol*, page 107, 1980.

[I2] Comorosan S. On a possible biological spectroscopy. *Bull Math Biol*, page 419, 1975.

Books related to TGD

[K1] Pitkänen M. Topological Quantum Computation in TGD Universe. In *Quantum - and Classical Computation in TGD Universe. https://tgdtheory.fi/tgdhtml/Btgdcomp.html*. Available at: `https://tgdtheory.fi/pdfpool/tqc.pdf`, 2015.

[K2] Pitkänen M. Basic Extremals of Kähler Action. In *Physics in Many-Sheeted Space-Time: Part I. https://tgdtheory.fi/tgdhtml/Btgdclass1.html*. Available at: `https://tgdtheory.fi/pdfpool/class.pdf`, 2023.

[K3] Pitkänen M. Bio-Systems as Super-Conductors: Part I. In *Bio-Systems as Self-Organizing Quantum Systems. https://tgdtheory.fi/tgdhtml/BbioSO.html*. Available at: https://tgdtheory.fi/pdfpool/superc1.pdf, 2023.

[K4] Pitkänen M. Bio-Systems as Super-Conductors: part II. In *Bio-Systems as Self-Organizing Quantum Systems. https://tgdtheory.fi/tgdhtml/BbioSO.html*. Available at: https://tgdtheory.fi/pdfpool/superc2.pdf, 2023.

[K5] Pitkänen M. Biological Realization of Self Hierarchy. In *Bio-Systems as Self-Organizing Quantum Systems. https://tgdtheory.fi/tgdhtml/BbioSO.html*. Available at: https://tgdtheory.fi/pdfpool/bioselfc.pdf, 2023.

[K6] Pitkänen M. Construction of Quantum Theory: M-matrix. In *Quantum TGD: Part I. https://tgdtheory.fi/tgdhtml/Btgdquantum1.html*. Available at: https://tgdtheory.fi/pdfpool/towards.pdf, 2023.

[K7] Pitkänen M. Dark Forces and Living Matter. In *Bio-Systems as Self-Organizing Quantum Systems. https://tgdtheory.fi/tgdhtml/BbioSO.html*. Available at: https://tgdtheory.fi/pdfpool/darkforces.pdf, 2023.

[K8] Pitkänen M. Dark Nuclear Physics and Condensed Matter. In *TGD and Nuclear Physics. https://tgdtheory.fi/tgdhtml/Bnucl.html*. Available at: https://tgdtheory.fi/pdfpool/exonuclear.pdf, 2023.

[K9] Pitkänen M. Negentropy Maximization Principle. In *TGD Inspired Theory of Consciousness: Part I. https://tgdtheory.fi/tgdhtml/Btgdconsc1.html*. Available at: https://tgdtheory.fi/pdfpool/nmpc.pdf, 2023.

[K10] Pitkänen M. TGD and Astrophysics. In *Physics in Many-Sheeted Space-Time: Part II. https://tgdtheory.fi/tgdhtml/Btgdclass2.html*. Available at: https://tgdtheory.fi/pdfpool/astro.pdf, 2023.

[K11] Pitkänen M. TGD and M-Theory. In *Topological Geometrodynamics: Overview: Part I. https://tgdtheory.fi/tgdhtml/Btgdview1.html*. Available at: https://tgdtheory.fi/pdfpool/MTGD.pdf, 2023.

[K12] Pitkänen M. TGD and Nuclear Physics. In *TGD and Nuclear Physics. https://tgdtheory.fi/tgdhtml/Bnucl.html*. Available at: https://tgdtheory.fi/pdfpool/padnucl.pdf, 2023.

[K13] Pitkänen M. TGD as a Generalized Number Theory: Infinite Primes. In *TGD as a Generalized Number Theory: Part I. https://tgdtheory.fi/tgdhtml/Btgdnumber1.html*. Available at: https://tgdtheory.fi/pdfpool/visionc.pdf, 2023.

[K14] Pitkänen M. The Relationship Between TGD and GRT. In *Physics in Many-Sheeted Space-Time: Part I. https://tgdtheory.fi/tgdhtml/Btgdclass1.html*. Available at: https://tgdtheory.fi/pdfpool/tgdgrt.pdf., 2023.

[K15] Pitkänen M. Was von Neumann Right After All? In *TGD and Hyper-finite Factors. https://tgdtheory.fi/tgdhtml/BHFF.html*. Available at: https://tgdtheory.fi/pdfpool/vNeumann.pdf, 2023.

[K16] Pitkänen M. Wormhole Magnetic Fields. In *Bio-Systems as Self-Organizing Quantum Systems. https://tgdtheory.fi/tgdhtml/BbioSO.html*. Available at: https://tgdtheory.fi/pdfpool/wormc.pdf, 2023.